N87-16746

D4-26
48P
49620

1986

NASA/ASEE SUMMER FACULTY FELLOWSHIP PROGRAM

MARSHALL SPACE FLIGHT CENTER

THE UNIVERSITY OF ALABAMA

GROWTH AND CHARACTERIZATION OF $Hg_{1-x}Zn_xSe$ SEMICONDUCTING ALLOYS

Prepared by:	R. N. Andrews, Ph.D.
Academic Rank:	Associate Professor
University and Department:	University of Alabama at Birmingham Department of Materials Engineering
NASA/MSFC:	
Laboratory:	Space Science Laboratory
Division:	Low Gravity Science
Branch:	Crystal Growth
MSFC Colleague:	S. L. Lehoczky, Ph.D. F. R. Szofran, Ph.D.
Date:	September 2, 1986
Contract No:	NGT 01-002-099 The University of Alabama

D4-26

GROWTH AND CHARACTERIZATION OF $Hg_{1-x}Zn_xSe$ SEMICONDUCTING ALLOYS

by

R. N. Andrews
Associate Professor of Materials Engineering
University of Alabama at Birmingham
Birmingham, Alabama

ABSTRACT

$Hg_{1-x}Zn_xSe$ alloys of composition x= 0.10 were grown in a Bridgman-Stockbarger growth furnace at translation rates of 0.3 and 0.1 μ m/sec. The axial and radial composition profiles were determined using precision density measurements and IR transmission-edge-mapping, respectively. A more radially homogeneous alloy was produced at the slower growth rate, while the faster growth rate produced more axially homogeneous alloys. These trends are consistent with other studies involving the influence of growth rate in similar II-VI semiconducting systems.

A determination of the electrical properties of the $Hg_{1-x}Zn_xSe$ samples in the temperature range 300K-20K was also made. Typical carrier concentrations were on the order of magnitude of 10^{18} cm^{-3}, and remained fairly constant as a function of temperature. A study was also made of the temperature dependence of the resistivity and Hall mobility. The effect of annealing in a selenium vapor on both the IR transmission and the electrical properties was determined. Annealing was effective in reducing the number of native donor defects and at the resulting lower carrier concentrations, charge carrier concentration was shown to be a function of temperature. Annealing caused the mobility to increase, primarily at the lower temperatures, and the room temperature resistivity to increase. Annealing was also observed to greatly enhance the % IR transmittance of the samples, from values of <0.5% before annealing to values >10% after annealing. This was due primarily to the effect of annealing on decreasing the charge carrier concentration.

ACKNOWLEDGMENTS

I would like to express my sincere appreciation to NASA/ASEE for providing me with the opportunity to participate a second year in the Summer Faculty Fellowship Program at Marshall Space Flight Center. The program directors, Ms. Ernestine Cothran and Dr. Fred Speer of NASA, and Dr. Mike Freeman of UA and Dina Conrad of UAH are to be commended for putting together and conducting an excellent program, one that was both informative and enjoyable. Their enthusiasm in the program was contagious and their friendship quite valued by this participant.

The author would also like to gratefully acknowledge the support, encouragement, and friendship of her colleagues, Dr. Alex Lehoczky and Dr. Frank Szofran of the Space Science Laboratory. Their continued interest and personal involvement in this project have served to make my past two summers at Marshall a very enjoyable and rewarding experience. Their many helpful discussions and assistance in varied phases of this work were invaluable. Special thanks go to Frank Szofran for his day-to-day help in the lab. His assistance, particularly with the Van der Pauw equipment for electrical property measurement, was vital to the successful conduction of this work.

Thanks are also extended to Ms. Sharon Cobb, a UAB graduate student who assisted in various phases of the experimental work on this project. Thanks also go to Dr. Ching Hua Su for his many helpful discussions, to Ms. Alice Dorries for help with the precision density measurements, and to Mr. Ron Harris for his assistance in sample prepartion and day-to-day laboratory operations. The assistance of Ms. Gretchen Perry in performing the IR Transmission analyses was also invaluable to the success of this project and her help is greatly appreciated.

Ms. Shirley Buford and Ms. Jeannie Cone are also due a special note of thanks for both their friendship and secretarial support this summer. Special thanks are also extended to Ms. Claudette Hanks for her patient assistance in the preparation of this report.

LIST OF FIGURES

Figure Number	Title	Page
1	Temperature Profile of Bridgman-Stockbarger Furnace. T_u =1000C, T_L = 645C (Scale Position = 0 corresponds to the bottom of the thermal barrier)	6
2	Axial Composition Profile of Alloy SC-5 (from precision density measurements)	9
3	Axial Composition Profile of Alloy SC-6 (from precision density measurements)	11
4	Wavenumber contour map of a sample taken 6.26cm from the tip of alloy SC-5	12
5	Wavenumber contour map of a sample taken 10.70cm from the tip of alloy SC-6	13
6	Carrier Concentration as a Function of Temperature for Sample SC6-10.70	16
7	Hall Mobility as a Function of Temperature for Sample SC6-10.70	17
8	Resistivity as a Function of Temperature for Sample SC6-10.70	18
9	Carrier Concentration as a Function of Temperature for Sample SC6-10.70 Annealed for 300 hours in Se Vapor	19
10	Hall Mobility as a Function of Temperature for Sample SC6-10.70 Annealed for 300 hours in Se Vapor	21
11	Resistivity as a Function of Temperature for Sample SC6-10.70 Annealed 300 hours in Se Vapor	22
12	% Transmittance vs. Wavenumber for the Central Region of Sample SC5-6.26 (as - grown)	23
13	Wavenumber Contour Map for Sample SC5-6.26	24

14	% Transmittance vs. Wavenumber for the Central Region of Sample SC5-6.26 (Annealed 96 hours in Se Vapor)	25
15	% Transmittance vs. Wavenumber for the Central Region of Sample SC5-6.26 (Annealed 300 hours in Se Vapor)	26
16	Carrier Concentration as a Function of Temperature for Sample SC6-7.70	31
17	Hall Mobility as a Function of Temperature for Sample SC6-7.70	32
18	Resistivity as a Function of Temperature for Sample SC6-7.70	33
19	Carrier Concentration as a Function of Temperature for Sample SC6-15.45	34
20	Hall Mobility as a Function of Temperature for Sample SC6-15.45	35
21	Resistivity as a Function of Temperature for Sample SC6-15.45	36
22	Carrier Concentration as a Function of Temperature for Sample SC5-2.11	37
23	Hall Mobility as a Function of Temperature for Sample SC5-2.11	38
24	Resistivity as a Function of Temperature for Sample SC5-2.11	39
25	Carrier Concentration as a Function of Temperature for Sample SC5-9.29	40
26	Hall Mobility as a Function of Temperature for Sample SC5-9.29	41
27	Resistivity as a Function of Temperature for Sample SC5-9.29	42

LIST OF TABLES

Table Number	Title	Page
1	Electrical Property Measurements of Selected Samples From Alloys SC-5 and SC-6	14

INTRODUCTION

Of considerable interest in the area of semiconductor research is the investigation of the growth and the characterization of II-VI semiconducting alloys. Several systems have been investigated and attention has been focused both on the various methods of formation of the alloys as well as on an evaluation of alloy properties.

The system investigated in this study was the HgSe-ZnSe system. Both HgSe and ZnSe crystallize in the zincblende structure and combine to form a continuous series of solid solutions. The melting point of HgSe is approximately 800C while that of ZnSe is 1700C, a fact which makes it difficult to produce alloys of high ZnSe composition. It is know that the variation of the lattice constant is linear, from a value of 6.086 angstroms for HgSe to a value of 5.6696 angstroms for ZnSe. HgSe is a perfect semimetal with an energy gap of -0.06 ev at 300K, while ZnSe is a semiconductor with an energy gap of 2.6 ev at 300K. Both linear and non-linear dependencies of the energy gap on composition have been reported in the literature.

This investigation focuses attention on both the growth and characterization of alloys in this system. The compositional uniformity, both radially and axially on Bridgman grown samples is evaluated as a function of growth rate. The electrical properties of the alloys, including carrier concentration, Hall mobility, and conductivity, in the temperature range 300-20K, are also determined. The effects of annealing $Hg_{1-x}Zn_xSe$ in a selenium vapor on both percent IR transmission and electrical properties is also evaluated.

OBJECTIVES

Work has been done by Nelson, et al (1) on the $Hg_{1-x}Cd_xSe$ system. In their work, it was observed that the electrical properties of the system, in particular the carrier concentration, were unstable as a function of time. The conduction - electron concentration with time and the electron mobility decreased simultaneously in samples which had been annealed in a dynamic vacuum.

In an attempt to stabilize the electrical properties, it was decided to use zinc additions in this investigation. It is believed that zinc may provide a stabilizing effect on the lattice and thus in turn would stabilize the electrical properties.

There were several objectives to this investigation. They were selected to systematically analyze the system and can be stated as follows:

1. Determination of the influence of growth rate on the compositional uniformity, both axially and radially, of Bridgman grown crystals of $Hg_{1-x}Zn_xSe$.

2. Determination of the electrical properties of $Hg_{1-x}Zn_xSe$ crystals in the temperature range 300-20K.

3. Evaluation of the effects of selenium - vapor annealing on both the % IR transmission and the electrical properties of $Hg_{1-x}Zn_xSe$ crystals.

4. Determination of the variation in electrical properties of samples of different compositions. (i.e. varying x).

BACKGROUND

The possibility of the formation of a continuous series of solid solutions in the HgSe - ZnSe system was first mentioned by Krucheamu (2) in 1962. Since that time, several studies have been performed on this system, with the primary emphasis being to evaluate the electrical properties of the system and to determination the band structure. Attention has also been focused on determining the scattering mechanisms operative over the temperature range 300-4.2K.

Kot and Simashkevich (3) appear to have been the first to synthesize $Hg_{1-x}Zn_xSe$ of various x compositions and upon subsequent x-ray analysis they found a linear relationship between composition and lattice constant. They produced both bulk specimens and thin films. The variation in electrical properties as a function of temperature appeared to be dependent on composition. For compositions up to 40% ZnSe, they observed a decrease in resistivity with increasing temperature. However, for compositions greater than 55% ZnSe, the resistivity was seen to increase as a function of increasing temperature. Electron concentrations were seen to vary from 3×10^{18} to 2×10^{17} cm^{-3}.

Potapov, et al (4) performed Shubnikov de Haas measurements of samples of $Hg_{1-x}Zn_xSe$ of composition x= 0.03-0.09. The oscillations were used to determine the effective election masses, the matrix elements of the interband interaction P, the energy gap, and the point of inversion of the energy band structure from an inverted semi-metal to a semiconductor. Their work showed that the effective mass of the electrons in $Hg_{1-x}Zn_xSe$ varied with Zn concentration and was minimal in the vicinity of x=0.06, indicating a point of inversion in gap energy corresponding to a composition of x= 0.06.

The band structure and carrier scattering mechanisms in $Hg_{1-x}Zn_xSe$ were studied by Gavaleshko and Khomyak (5). They prepared their alloys by direct melting in quartz ampoules with subsequent growth in a Bridgman furnace. As a result of their study, they concluded that in the range of carrier densities in their investigation, $n = 7 \times 10^{14} - 5 \times 10^{18}$ cm^{-3}, and at 77°K, scattering is dominated by optical and piezoacoustic phonons.

Potapov, et al (6) determined the magnetoresistances and the Hall effect of $Hg_{1-x}Zn_xSe$ samples with electron densities of 5×10^{17} cm^{-3} in the temperature range 1.6 to 20K. They also studied the temperature dependences of the electrical conductivity and Hall effect in the range 4.2 to 300K. They correlated changes in mobility with temperature to changes in scattering mechanisms. In their work, it was determined that the transition point from a semimetal to a semiconductor was in the vicinity of x = 0.06 to x = 0.07. With increasing temperature, and x = 0.06 or 0.07, the electrical conductivity was shown to increase by almost a factor of seven in cooling from 300 - 30K, while the mobility increased by a factor exceeding ten. The electron mobility remained constant in the temperature range 4.2 - 30K, thus it was assumed that the dominant scattering mechanism was due to ionized impurities. In the temperature

range 30-90K, mobility obeyed $\mu \alpha T^{-1}$, which corresponds to scattering of electrons by acoustic phonons. At T > 90K, the dependence was $\mu \alpha T^{-5/2}$, indicating scattering by optical phonons.

The dependence of mobility on composition and temperature in $Hg_{1-x}Zn_xSe$ crystals of compositions ranging from x values of $0 \leq X \leq 0.15$ was determined by Gavaleshko, et al (7). In their study they determined a relationship between band gap and composition for $0 \leq X \leq 0.15$ for both 77K and 300K. Their calculations showed that the best fit to their data could be expressed by the following equation:

$$Eg(x,T) = -0.244 + 6.7253x - 24.939x^2 - 101.82x^3 + 883.9633x^4 +$$

$$(6 - 81.56x - 511.691x^2 - 116x^3 - 7021X^4) \times 10^{-4} T$$

where $0 \leq x \leq 0.15$ and $50 \leq T \leq 300K$. They also obtained an expression for the band gap vs composition at T = 77K assuming a linear variation of Eg with T. This is given by:

$$Eg(x,T) = -0.244 + 3.064x + (6-11x) \times 10^{-4} T$$

In looking at the temperature dependence of mobility, Gavaleshko, et al (7) concluded that the dominating scattering mechanisms in $Hg_{1-x}Zn_xSe$ solid solutions are by impurity ions and polar optical phonons.

In subsequent work, Gavaleshko et al (8) performed an investigation of the infrared spectra of $Hg_{1-x}Zn_xSe$ alloys and the results were used to find the effective masses of these solid solutions as a function of composition and carrier density. The Bridgman growth technique was used in this work to prepare samples, with subsequent annealing performed to control carrier concentration. They determined Hall mobilities and found that the mobility varied from 2.2×10^4 cm^2 v^{-1} sec^{-1} for HgSe, to 2-3 x 10^3 cm^2 v^{-1} sec^{-1} for a composition of x = 0.75, reaching its maximum value of 2×10^5 cm^2 v^{-1} sec^{-1} for a composition of x = 0.06. From their work, they also determined that the transition from an inverted band structure to a semiconductor in $Hg_{1-x}Zn_xSe$ alloys occurs in the range $x \simeq 0.02 - 0.05$.

Leibler et al (9) investigated $Hg_{1-x}Zn_xSe$ alloys and measurements were made of the electrical conductivity and electron concentration as a function of temperature for alloys of composition $x \leq 0.45$. For all compositions studied, conductivity was seen to decrease as temperature increased. The Hall coefficient was observed to be either independent of temperature or increased slightly as the temperature decreased.

EXPERIMENTAL PROCEDURE

Alloy Preparation

All alloys in this investigation were prepared using at least 5 - nine's pure elements. They were prepared in accordance with previously reported alloy preparation techniques (10). Briefly, the elements were loaded and sealed in evacuated thick wall quartz ampoules. The ampoules were then placed in a rocking furnace and heated to 1150C to pre-react the elements. An intermittent hold at 500-600C for approximately two days was included to allow sufficient time for diffusion to take place. The slow heating procedure and the long soak time at low temperature was suggested by Kot et al (3) for the processing of alloys in this system.

Crystal Growth

The alloys were subsequently grown in a Bridgman - Stockbarger growth furnace at pre-selected growth rates and under controlled thermal conditions. The specifics of the furnace design and operation are described in detail by Lehoczky et al in Ref (11). Briefly, the ampoule remains stationary in this method and the furnace assembly, which consists of two resistively heated tubular furnaces, translates upwards. This gradually moves the ampoule containing the molten alloy from the hot furnace into the cooler region, thus causing solidfication of the alloy. Utilization of heat pipes in both the upper and lower furnaces produced well defined heat zones. In this study, the upper zone was at 1000C and the lower zone was at 645C with a 2.4cm thermal barrier between the two zones. The temperature profile which was obtained in the empty furnace and which was used in all growth processes in this study is shown in Figure 1.

Precision Density Measurements

Since the variation in lattice constant for $Hg_{1-x}Zn_xSe$ varies linearly with x, from a value of 6.086 angstroms for HgSe to a value of 5.6696 angstroms for ZnSe, the mass density of $Hg_{1-x}Zn_xSe$ will also vary linearly with x since both compounds crystallize in the zineblende structure. Thus, precision density measurements can be made in this system and used to accurately determine alloy composition. The precision density measurements were made in accordance with the procedure outlined by Bowman and Schooner (12). These measurements were made on thin slices (0.75 - 1mm thick) taken along the length of each crystal and this compositional data was used to determine the axial compositional uniformity of the crystal.

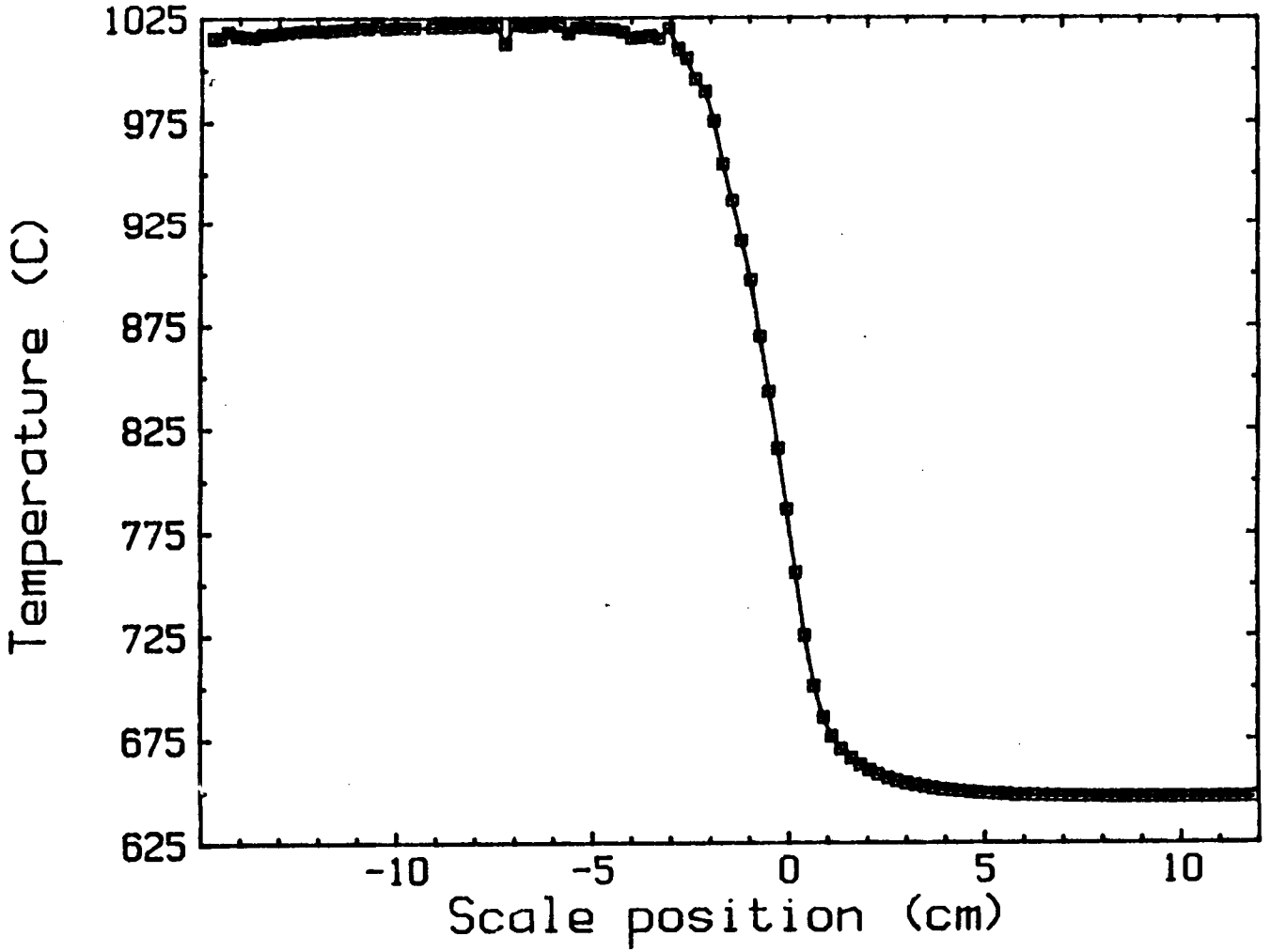

Figure 1. Temperature Profile of Bridgman-Stockbarger Furnace. T_u =1000C, T_L = 645C (Scale Position = 0 corresponds to the bottom of the thermal barrier)

IR Transmission-Edge Mapping

IR transmission-edge mapping was used to determine both the radial compositional uniformity and the percent IR transmittance on slices taken along the length of each crystal. In this method, a map of cut-on wavenumber or wavelength, as the sample goes from being opaque to transparent to the infrared is made on the crystal slice. In many other II - VI systems, where the variation of energy gap with composition (x) is known, the wavenumber corresponding to this particular gap energy can be converted to a corresponding x value and a radial compositional profile of the slice can obtained. However, since the exact variation of Eg with x in the $Hg_{1-x}Zn_xSe$ system is unknown at this time, a wavenumber contour map was used to evaluate radial homogeneity. Also, the transmission edge-mapping technique allows the maximum % IR transmission through a crystal slice to be determined.

Electrical Property Measurements

The electrical properties of samples taken from the crystals grown in this investigation were measured using the Van der Pauw technique (13). Electrical leads which were 2 mil diameter copper wire were soldered to circular wafers taken from the samples. Indium solder was used to achieve an ohmic contact. Before the leads were attached, the samples were ground and etched in a solution of 5% bromine in methanol and rinsed in methanol.

The automated Van der Pauw facility used in this investigation was capable of electrical property measurement in the temperature range 300K - 20K and used a 5000 gauss magnetic field. The Hall coefficient, electrical resistivity, carrier concentration, and Hall mobility, were all determined or calculated from the results of these measurements.

Selenium - Vapor Annealing

In order to vary the concentration of defect electrons in the $Hg_{1-x}Zn_xSe$ crystals, selected slices taken from the as-grown crystals were annealed in a selenium vapor at 260C. The crystal slices were sealed in evacuated quartz tubes along with several pieces of selenium and annealed for various times. Annealing times ranged from 96 hours to over 300 hours.

PROGESS TO DATE

To date, two alloys of composition x = 0.10 have been successfully grown. These are designated SC-5 and SC-6 and were grown at furnace translation rates of 0.30 μm/sec and and 0.10 μm/sec, respectively. An alloy of composition x = 0.10 has been prepared (SC-13) and is currently being grown at a translation rate of 0.03 μm/sec. Also, an alloy of composition x = 0.08 has been prepared and is being grown at a translation rate of 0.1 μm/sec. This sample, when analyzed, will help provide information on the influence of varying compositon (x) on the electrical properties of $Hg_{1-x}Zn_xSe$ alloys.

The axial compositional uniformity of SC-5 and SC-6 is being determined using precision density measurements of slices taken along the length of each crystal. Also, the radial compositional uniformity of SC-5 and SC-6 is being determined using IR transmission-edge mapping of slices taken along the length of each crystal.

Electrical property measurements, including carrier concentration, Hall mobility and resistivity have been determined as a function of temperature for several samples taken from SC-5 and SC-6.

The effects of selenium-vapor annealing on the % IR transmission and on the electrical properties have also been determined for several samples from SC-5 and SC-6.

RESULTS AND DISCUSSION

Axial Compositional Uniformity

One of the objectives of this study was to determine the influence of growth rate on the axial compositional uniformity of $Hg_{1-x}Zn_xSe$ crystals. Samples SC-5 and SC-6 were grown under identical thermal conditions and differred only in their growth rate, SC-5 being grown at 0.3 μm/sec and SC-6 being grown at 0.1 μm/sec. Therefore, a comparison of their axial compositional profiles should give an indication of the influence of growth rate on axial homogeneity. As can be seen in Figure 2, which is a preliminary plot of composition (as determined from precision density measurements) as a function of distance from the ampoule tip of crystal SC-5, the general trend in the profile is characteristic of that generally observed for faster grown crystals. That is, there appears to be a fairly large distance over which steady state growth occurred. Another observation which can be made from this profile is that the initial and final transients appear to be rather small, indicating that the effective diffusion coefficient may be smaller in this system than in other similar II - VI systems.

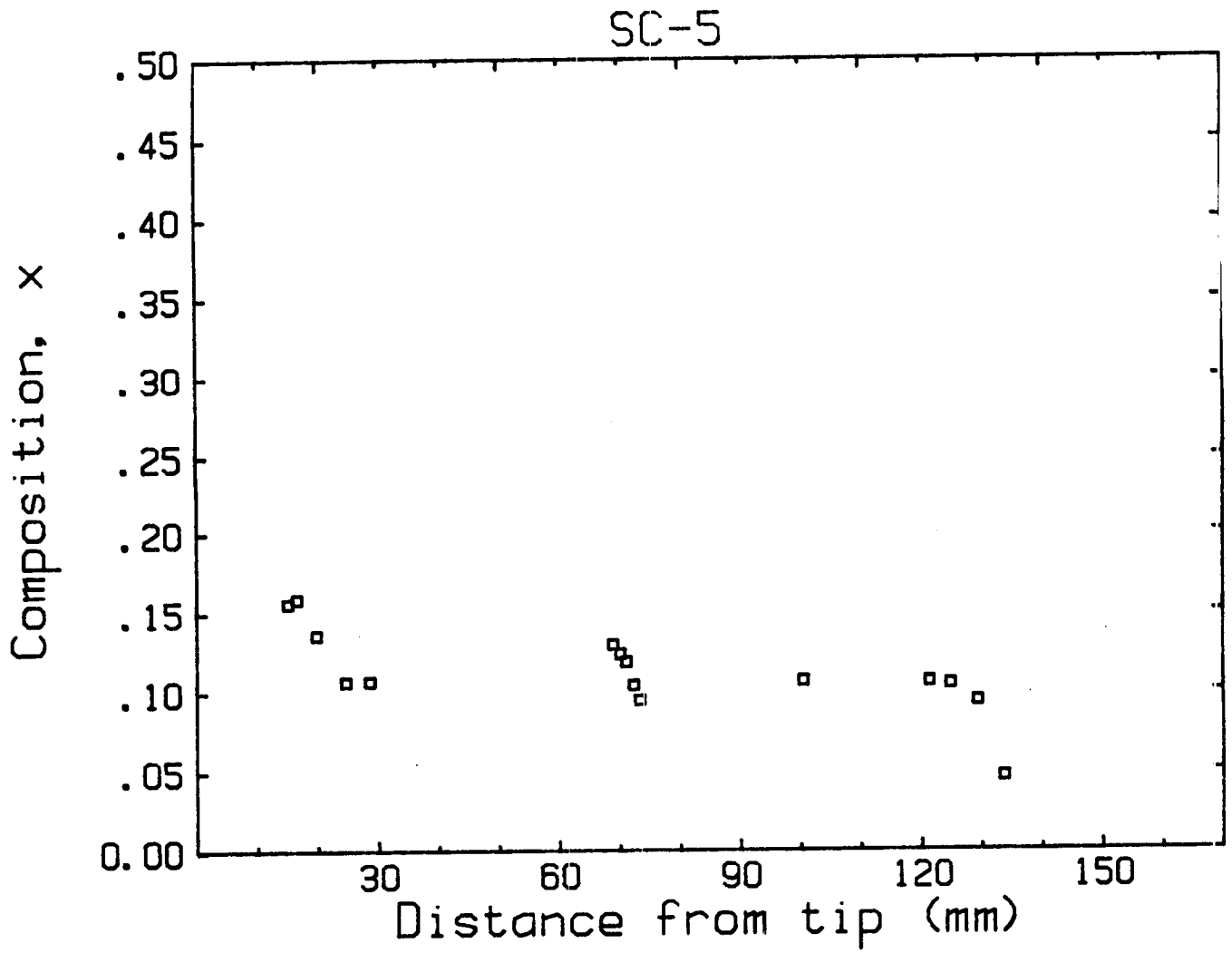

Figure 2. Axial Composition Profile of Alloy SC-5 (from precision density measurements)

In looking at Figure 3, it is seen that the axial composition profile for SC-6 is more characteristic of a slowly grown crystal, that is, there does not appear to be as large a region of uniform composition over which steady state growth occured.

Again, the compositional data plotted in both Figures 2 and 3 are preliminary at this time. Additional data points in the profiles are being determined as well as duplicate density measurements and hence compositional values being determined on samples already run and shown on these plots.

Radial Compositional Uniformity

As mentioned previously in this report, infrared transmission edge mapping was used to determine the radial uniformity of thin slices taken along the length of each crystal. Since the exact relationship between wavenumber or gap energy and composition in this system is not known, radial homogeneity will be discussed in terms of the variation in wavenumber across a slice.

Due to the high carrier concentrations in both as-grown SC-5 and as-grown SC-6, many times a radial slice taken from the crystals did not transmit over the whole area of the slice. This made it difficult to get an indication of the homogeneity of the slice. Therefore, samples of SC-5 and SC-6 which had been annealed to reduce their carrier concentration were used for comparison to indicate the influence of growth rate on the radial uniformity. Figure 4 shows the wavenumber contour map of a crystal slice taken 6.26 cm from the tip of alloy SC-5. The slice has been annealed in a selenium vapor for approximately 260 hours. In looking at the variation of wavenumber across the slice, a variation from 1190 to 2128 is observed, a difference of 938 wavenumbers. In comparison, Figure 5 shows the wavenumber contour map of a slice taken 10.70 cm from the tip of SC-6, the slowly grown alloy (0.1 μ m/sec.). This slice was annealed approximately 300 hours. The wavenumber variation across this slice is from 1225 to 1383, a difference of only 258 wavenumbers. Thus, although we do not have a direct comparison of radial compositional uniformity between SC-5 and SC-6 in terms of compositional profiles, the wavenumber profiles, which are related to compositional profiles, indicate that a slower growth rate produces a more radially homogeneous material.

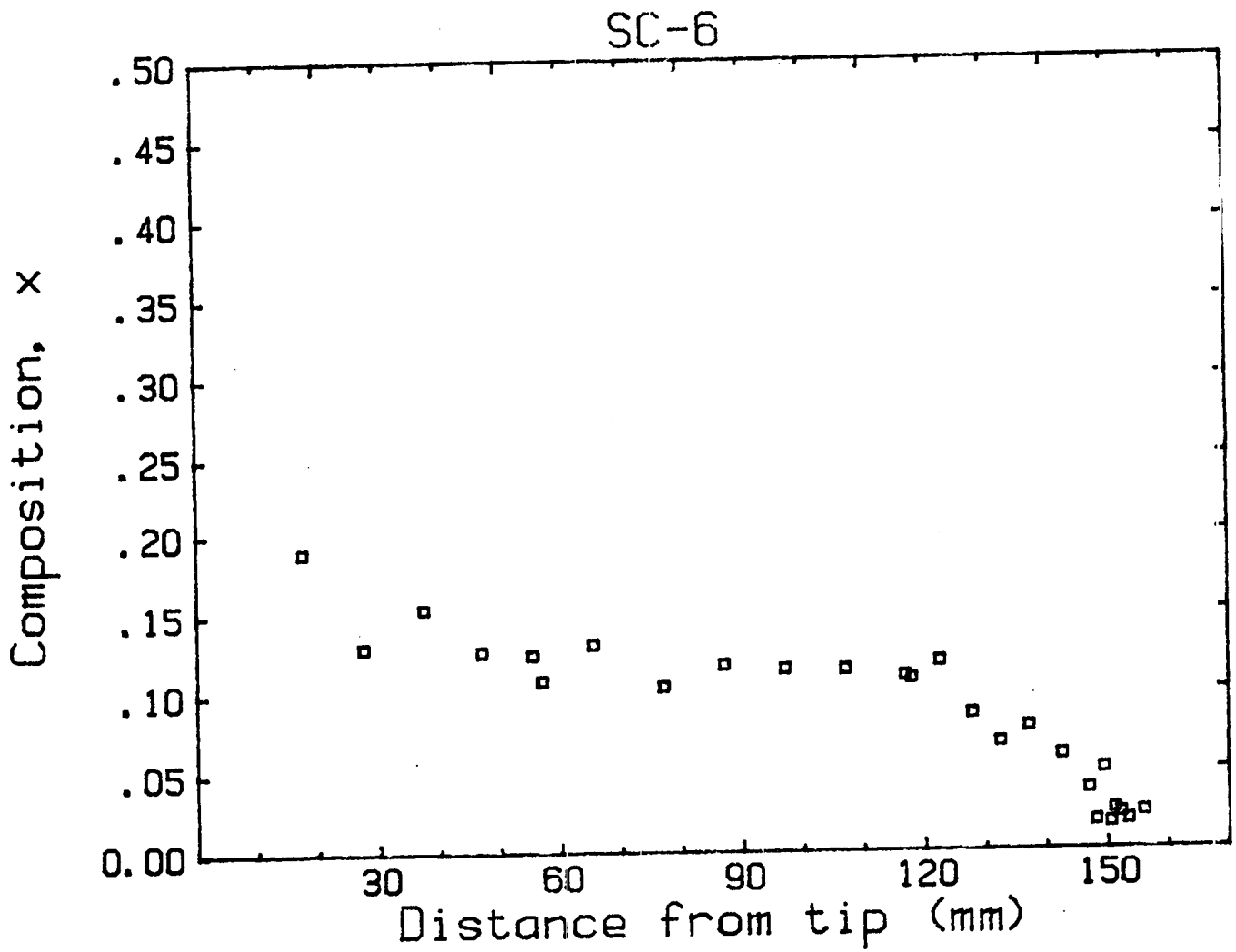

Figure 3. Axial Composition Profile of Alloy SC-6 (from precision density measurements)

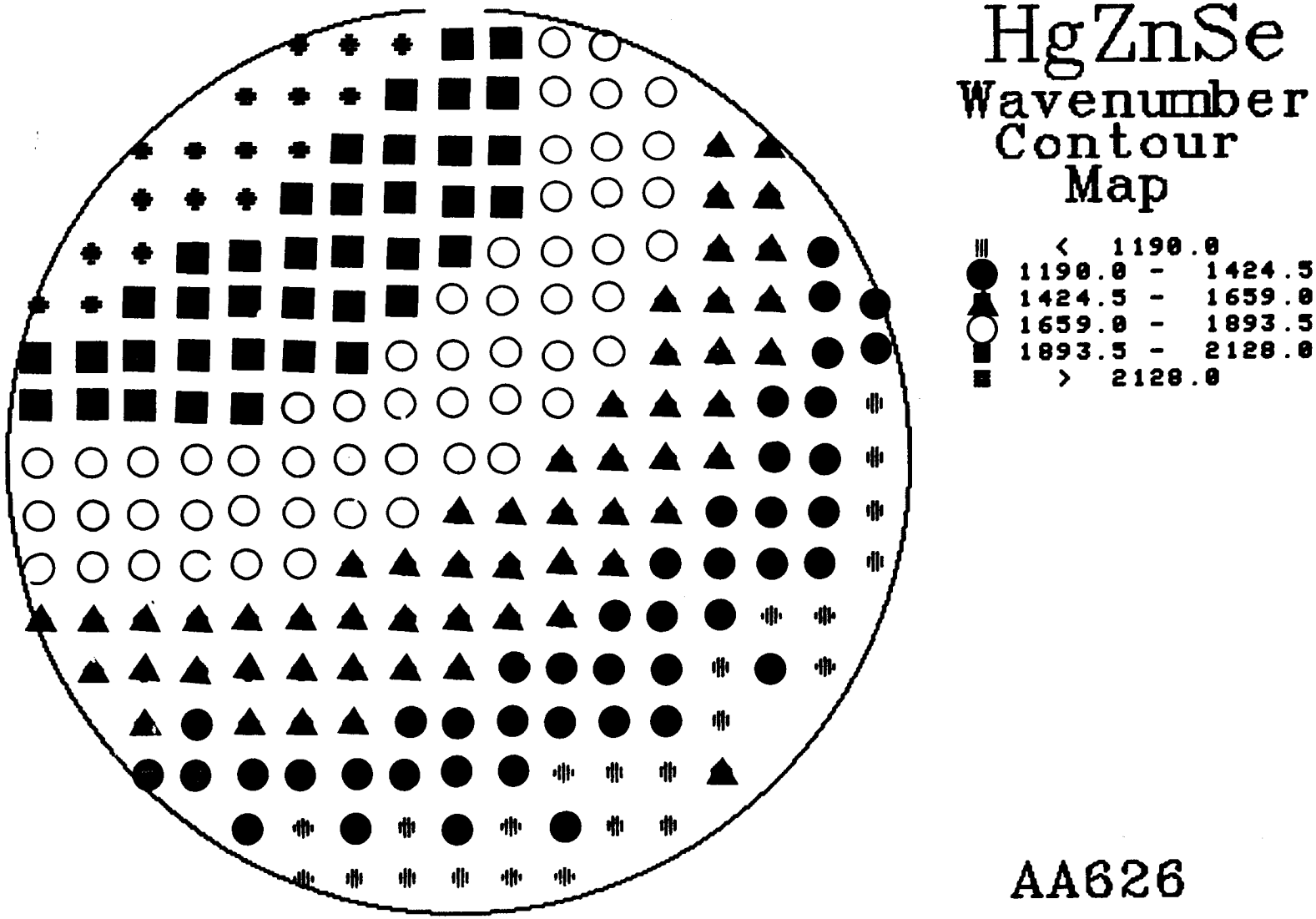

Figure 4. Wavenumber contour map of a sample taken 6.26cm from the tip of alloy SC-5

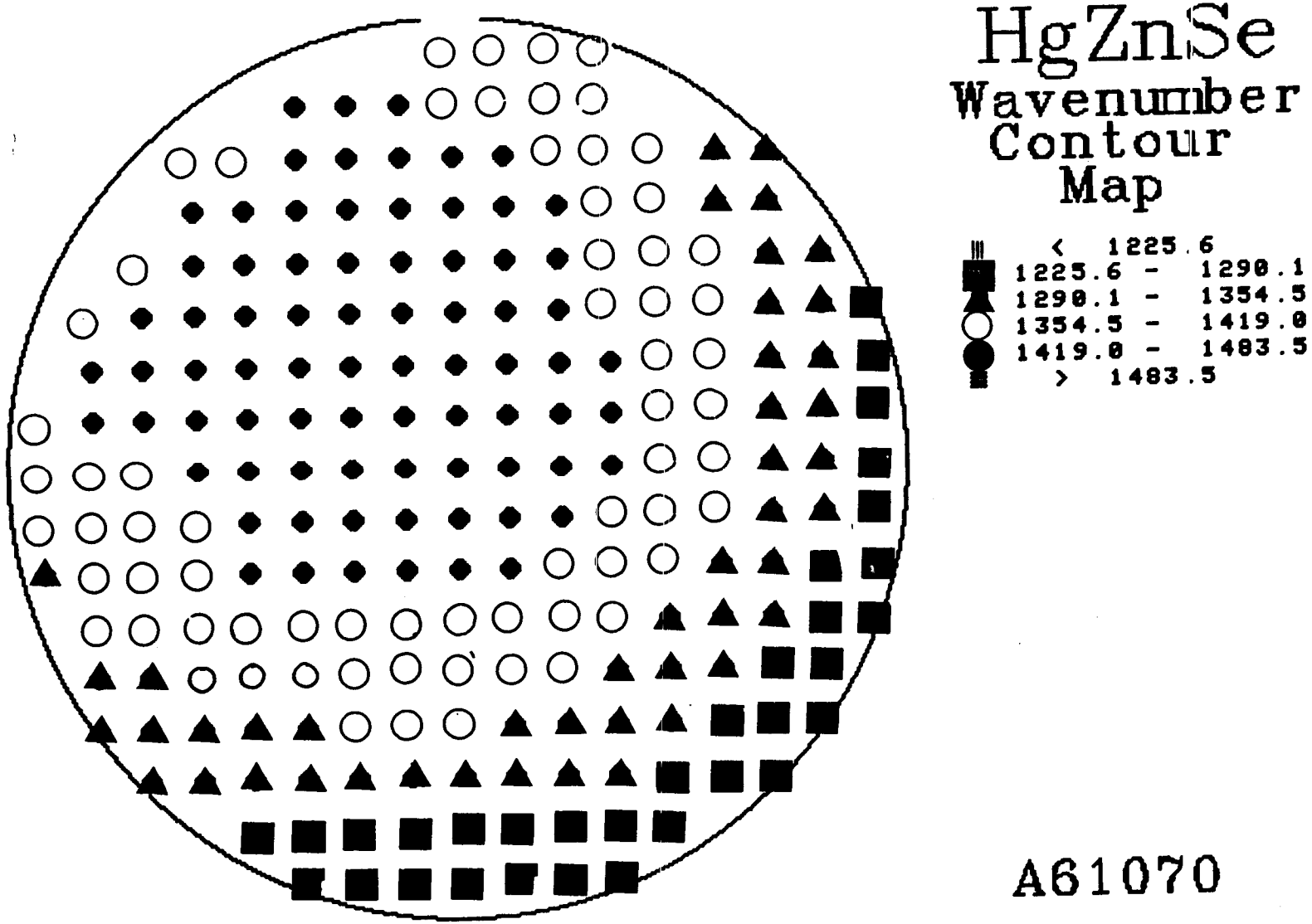

Figure 5. Wavenumber contour map of a sample taken 10.70cm from the tip of alloy SC-6

Electrical Property Measurements

The electrical properties of several slices taken from SC-5 and SC-6 were determined using the Van der Pauw method mentioned previously. Table 1 lists the values obtained in these measurements.

Table 1

Electrical Property Measurements of Selected Samples
From Alloys SC-5 and SC-6

Sample	n	μ*		ρ*	
SC6 7.70	1.7E + 18	2.4E+3	9E+3	1.6E-3	4E-4+
SC6 10.70	1.6E + 18	4.0E+3	1.8E+4	1.0E-3	2.8E-4
SC6 15.45	2.4E + 18	7.0E+3	1.7E+4	4.0E-4	1.8E-4
SC5 2.11	1.3E + 18	4.0E+3	1.7E+4	1.2E-3	3.0E-4
SC5 9.29	1.6E + 18	4.0E+3	1.7E+4	1.0E-3	2.9E-4

* Values correspond to the variation from 300K to 20K

\+ Measurements from 300K to 60K

All samples are in the as-grown condition and do not reflect any subsequent treatment such as selenium vapor annealing. The values which were determined were carrier concentration in cm^{-3}, Hall mobility in $cm^2/V\text{-sec}$, and resistivity in ohm-cm. All measurements were taken between 300 and 20K, except as noted in the Table. The carriers being measured are electrons in this material since $Hg_{1-x}Zn_xSe$ is an n-type material.

As a representative example of the trends which were observed, the carrier concentration, Hall mobility, and resistivity as a function of temperature for a sample taken 10.70 cm from the tip of alloy SC-6 are shown in Figure 6, 7, and 8 respectively. For completeness, all the plots of the electrical properties as a function of temperature for other samples which were analyzed to date in this study are included in Appendix I.

As can be seen, both in Table 1 and in Figure 6, the carrier concentration is on the order of magnitude of 10^{18} cm^{-3} in the as-grown condition and appears to be fairly constant as a function of temperature. This behavior as a function of temperature is to be expected at this high of a carrier concentration since the large number of defect carriers tend to mask any decrease in intrinsic charge carriers which may be expected to occur as the temperature decreases.

Table 1 and Figure 7 show the general trend observed in the Hall mobility as a function of temperature. As would be expected, the mobility decreases as temperature increases due to a combination of various scattering mechanisms which are operative and which tend to limit electron mobility.

Also, Figure 8 and Table 1 show the general trend observed in resistivity as a function of temperature. Considering the general independence of carrier concentration with temperature and the decrease in mobility with increasing temperature, the resistivity shows the expected general increase with increasing temperature.

Effects of Annealing on Electrical Properties

In order to observe the effect which selenium vapor annealing has on the electrical properties, a comparison was made of the electrical properties of SC-6 10.70 both before, and after annealing for approximately 300 hours. Figure 9 shows the variation in carrier concentration as a function of temperature after annealing. As can be seen, the carrier concentration is lower at all temperatures in the annealed sample in comparison to the SC-6 10.70 unannealed sample (Figure 6). This indicates that annealing effectively reduced the concentration of native donor defects, believed to be mercury interstitials in the case of $Hg_{1-x}Zn_xSe$ crystals. Also, as seen in Figure 9, the carrier concentration is seen to vary as a function of temperature, decreasing from a value of approximately 1.6×10^{18} at 300K to a value of 2.2×10^{17} at 20K. In this material, with a lower carrier concentration, it is now possible to observe the thermal depopulation characteristic of the intrinsic behavior of semiconductors with decreasing temperature.

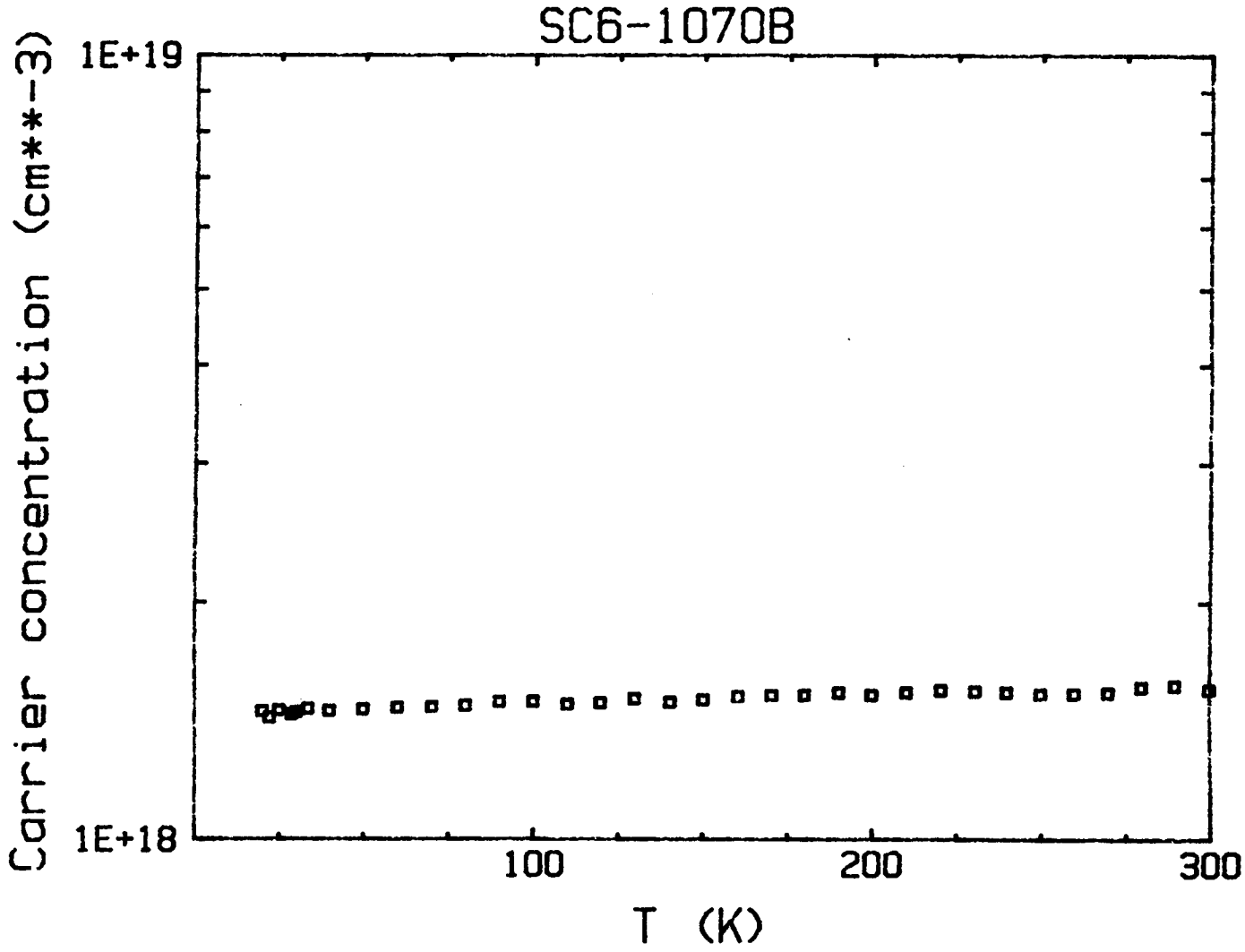

Figure 6. Carrier Concentration as a Function of Temperature for Sample SC6-10.70

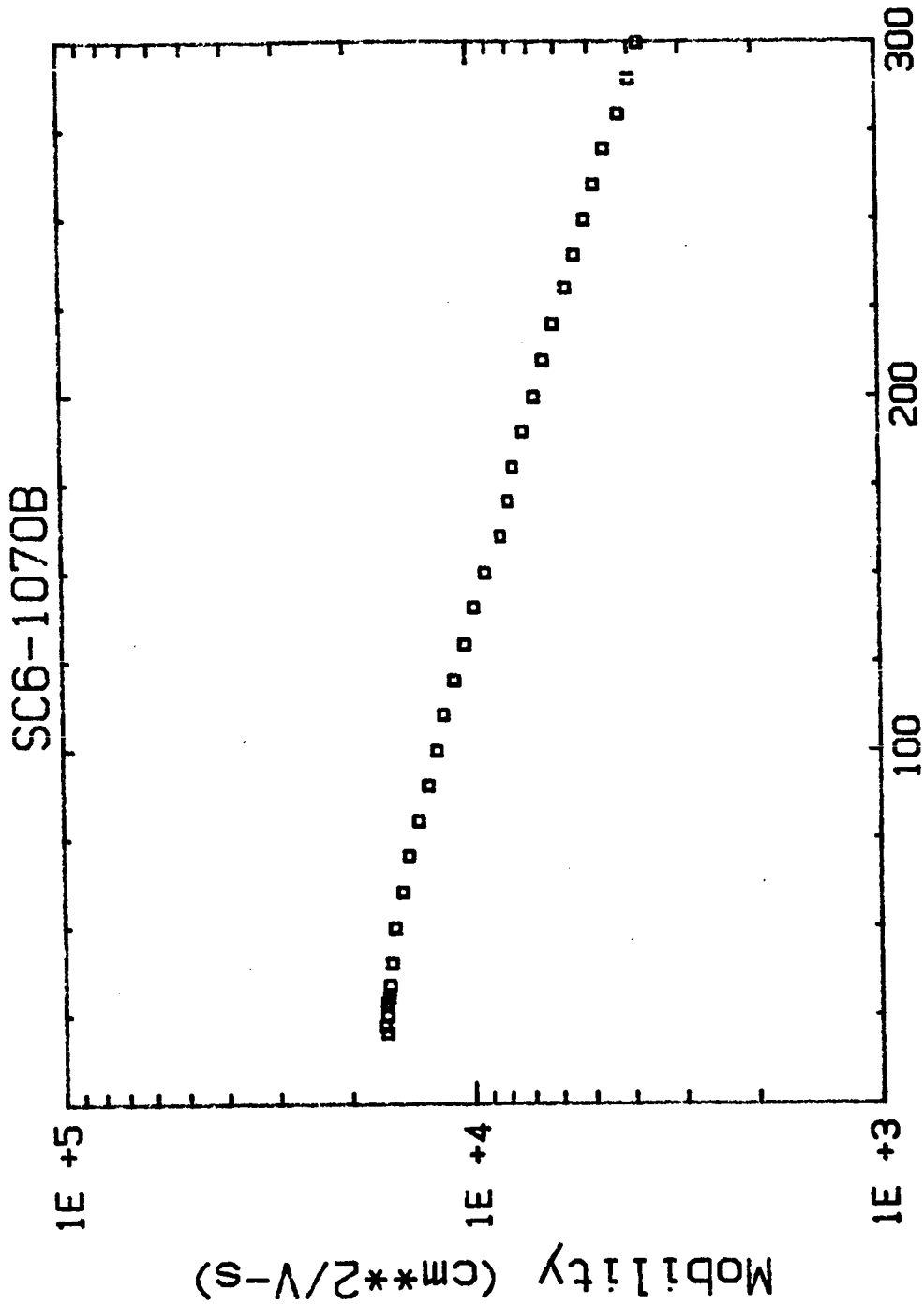

Figure 7. Hall Mobility as a Function of Temperature for Sample SC6-10.70

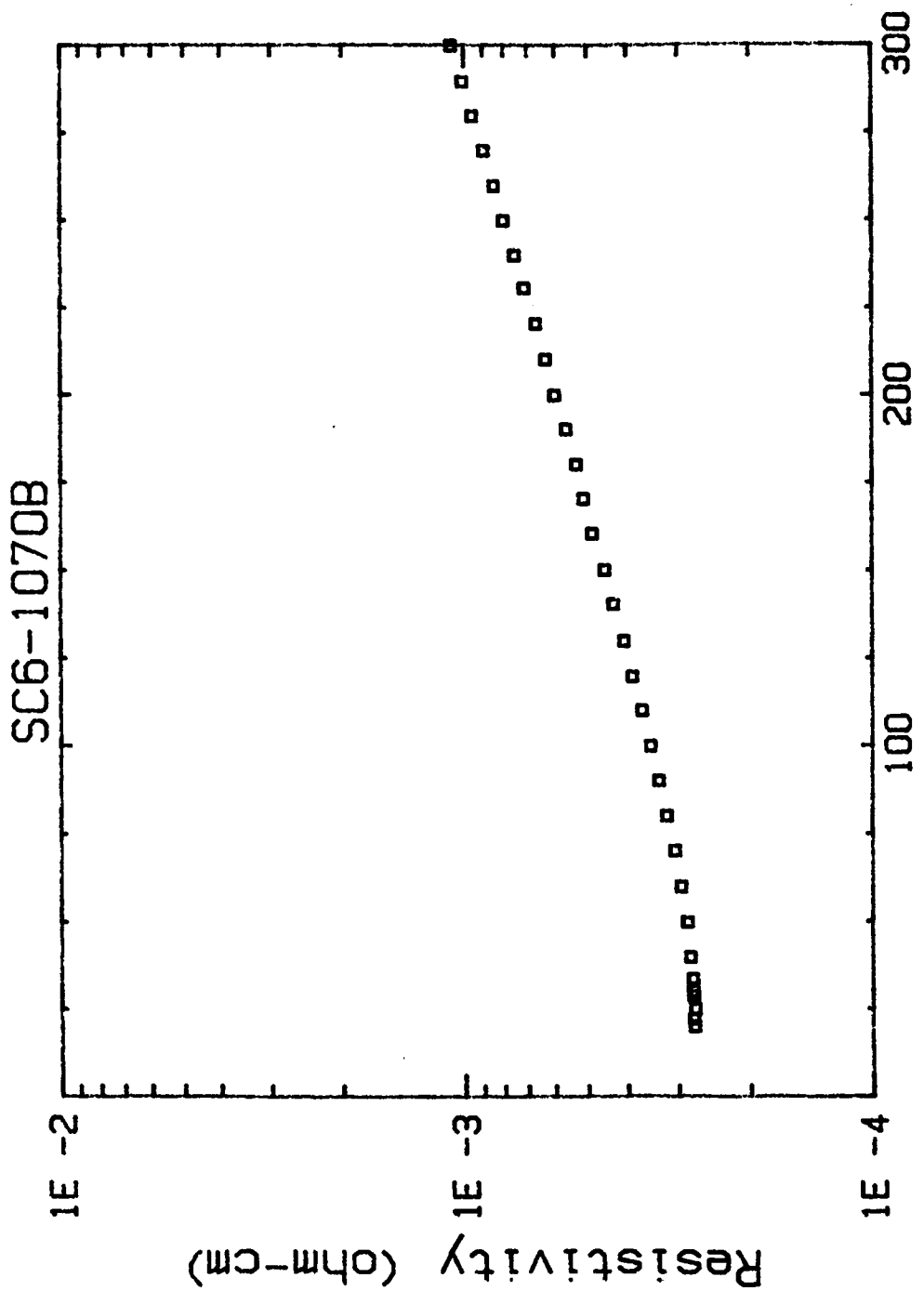

Figure 8. Resistivity as a Function of Temperature for Sample SC6-10.70

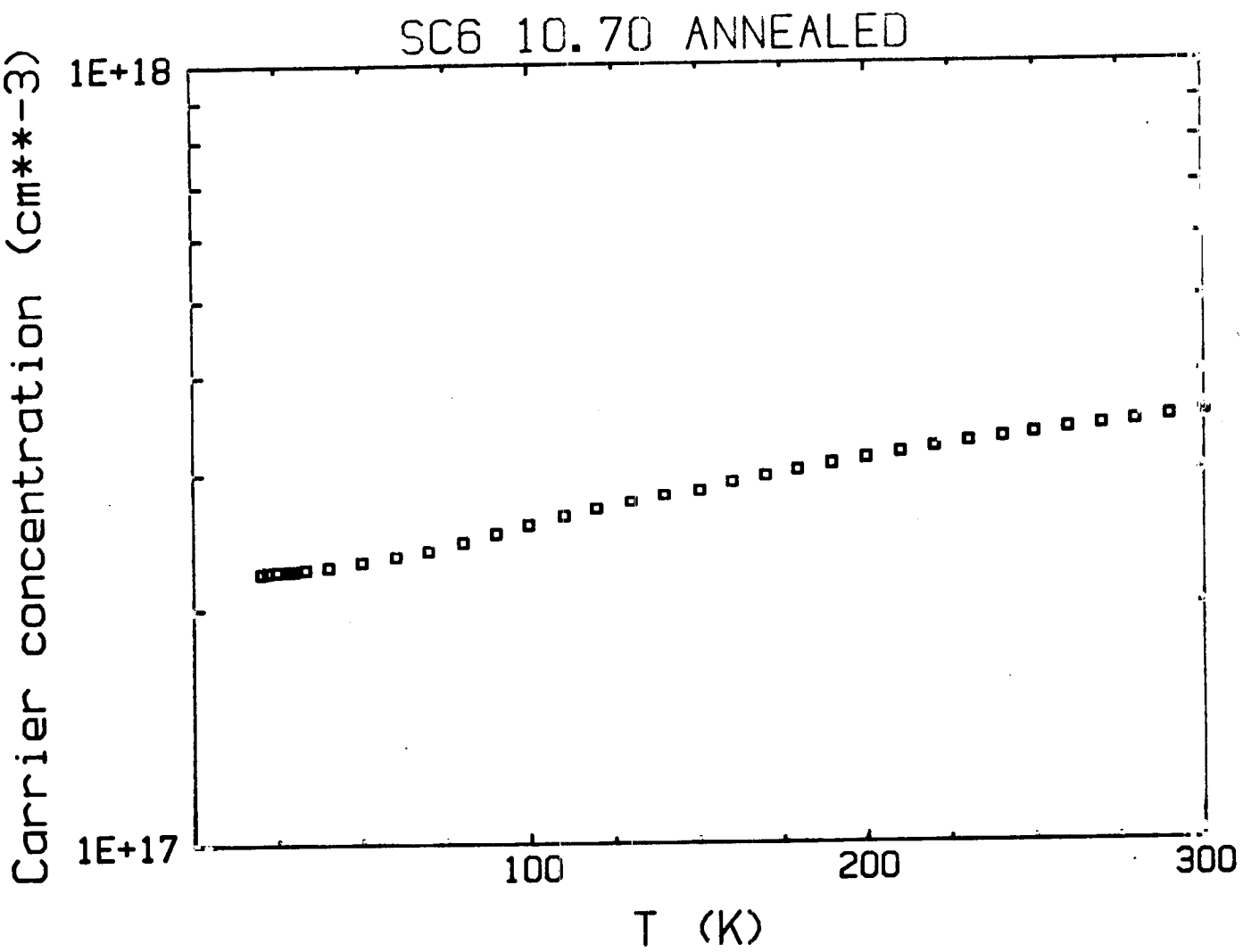

Figure 9. Carrier Concentration as a Function of Temperature for Sample SC6-10.70 Annealed for ∿ 300 hours in Se Vapor

Figure 10 shows the Hall mobility as a function of temperature in the annealed SC-6 10.70 sample. In comparing this with Figure 7, it can be seen that the initial mobility at room temperature is approximately the same, with a value of 4×10^3 $cm^2/v\text{-}sec$. This is to be expected because the primary effects on mobility at higher temperatures are due to intrinsic scattering processes. However, at lower temperatures, it is seen that the mobility in the annealed sample increases to a value of 9×10^5 $cm^2/v\text{-}sec$ at 20K in comparison to a value of 1.8×10^4 $cm^2/v\text{-}sec$ at 20K for the unannealed sample. Since extrinsic scattering processes are more dominant at lower temperatures, a higher mobility would be expected in a material with a lower defect concentration.

In Figure 11, the resistivity of the annealed SC-6 10.70 sample is shown as a function of temperature. The same general trend as a function of temperature is seen as in the unannealed sample (Fig. 8), however the room temperature resistivity is higher, with a value of 4×10^{-3} ohm-cm as compared to 1×10^{-3} ohm-cm for the unannealed sample. This would be expected due to the lower carrier concentration in the annealed sample. The low temperature resistivity in the annealed sample is, however, approximately equivalent to the low temperature resistivity in the unannealed sample. Although the carrier concentration is lower in the annealed sample, the large increase in low temperature mobility tends to have a compensating effect.

Effects of Annealing on the % IR Transmittance

Selenium - vapor annealing was shown to greatly enhance the % IR transmittance of samples of $Hg_{1-x}Zn_xSe$. A plot of the % IR transmittance versus wavenumber taken for several points near the center of a slice taken 6.26 cm from the tip of alloy SC-5 is shown in Figure 12. The maximum transmission in this area of the slice is approximately 0.5%. In fact, if one were to look at the radial wavenumber contour map as seen in Figure 13, this sample was opaque to the infrared over a large portion of the sample. After annealing in a selenium vapor for 96 hours, the % IR transmittance vs wavenumber plot for the same area of the sample as before is shown in Figure 14. As can be seen, the maximum transmittance in this area has increased to approximately 8%. Going one step further, when this same sample was annealed an additional 168 hours, the % IR transmittance plot for the same region of the sample, as seen in Figure 15, shows a maximum transmittance of approximately 10%. Also, as the full radial wavenumber profile shows, the % IR transmittance through the entire slice has increased, as seen previously in Figure 4.

Thus, it is fairly clear that annealing is effective in reducing the number of native donor defects, thus improving the % IR transmittance characteristics of $Hg_{1-x}Zn_xSe$ crystals.

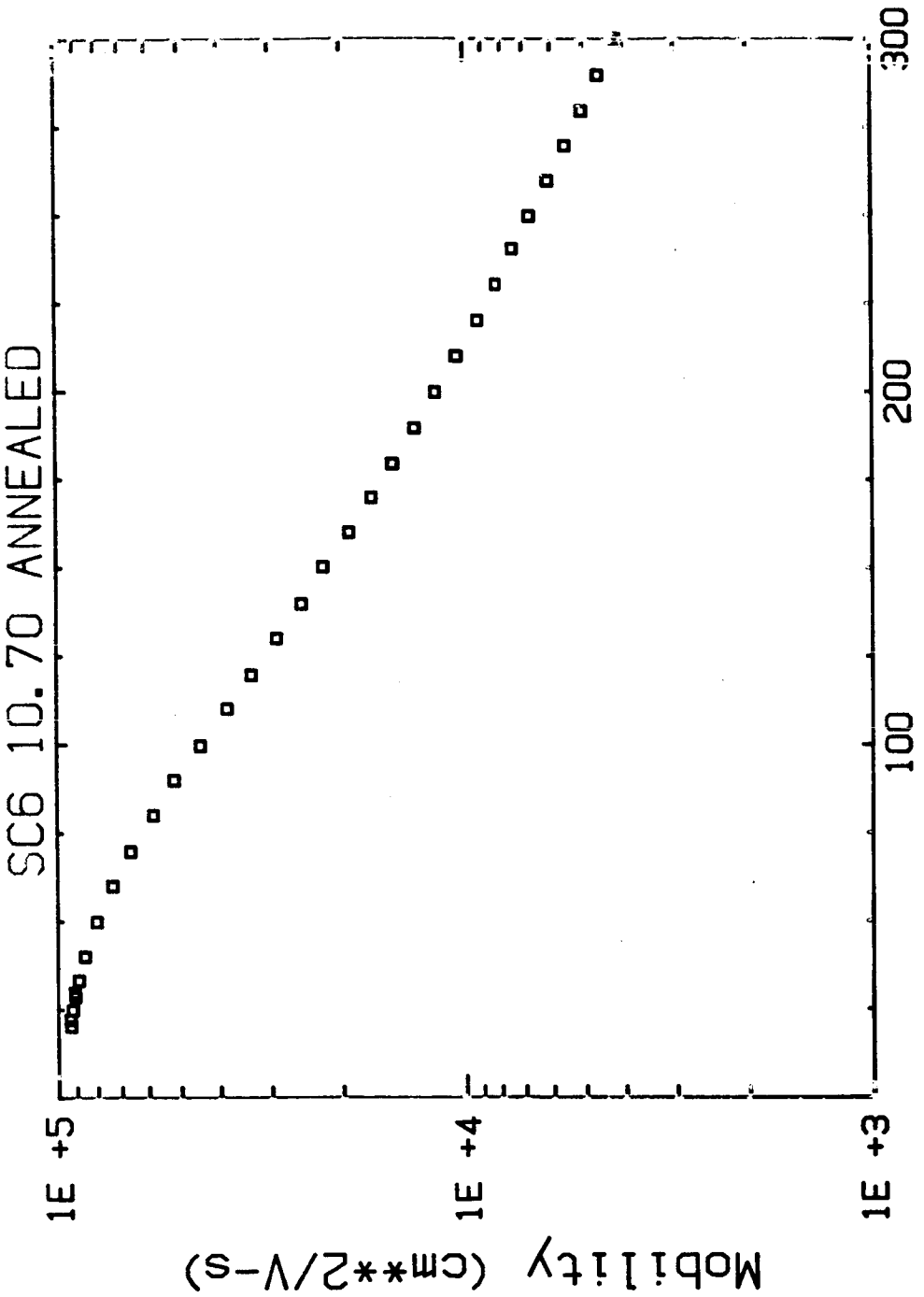

Figure 10. Hall Mobility as a Function of Temperature for Sample SC6-10.70 Annealed for ∿ 300 hours in Se Vapor

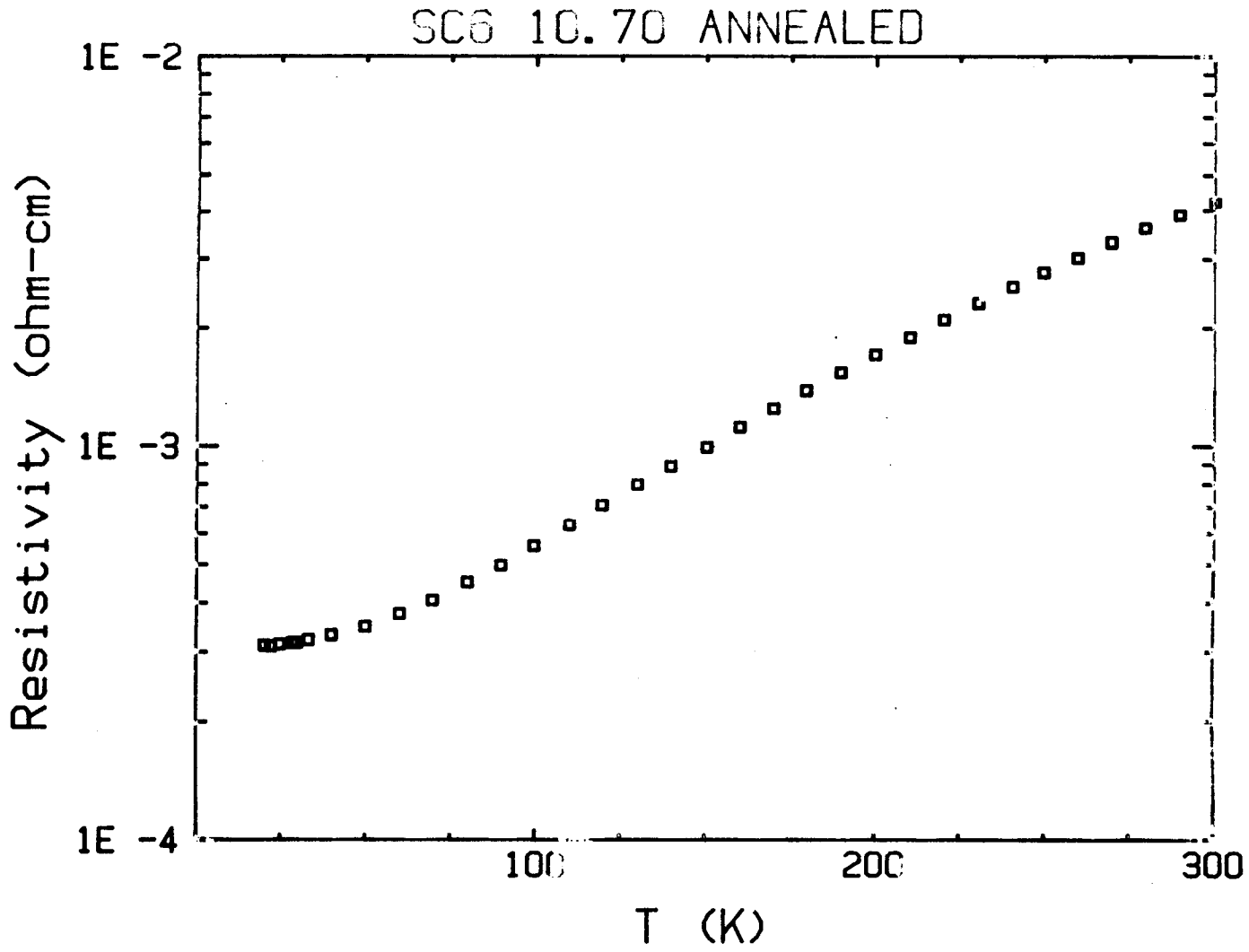

Figure 11. Resistivity as a Function of Temperature for Sample SC6-10.70 Annealed ~ 300 hours in Se Vapor

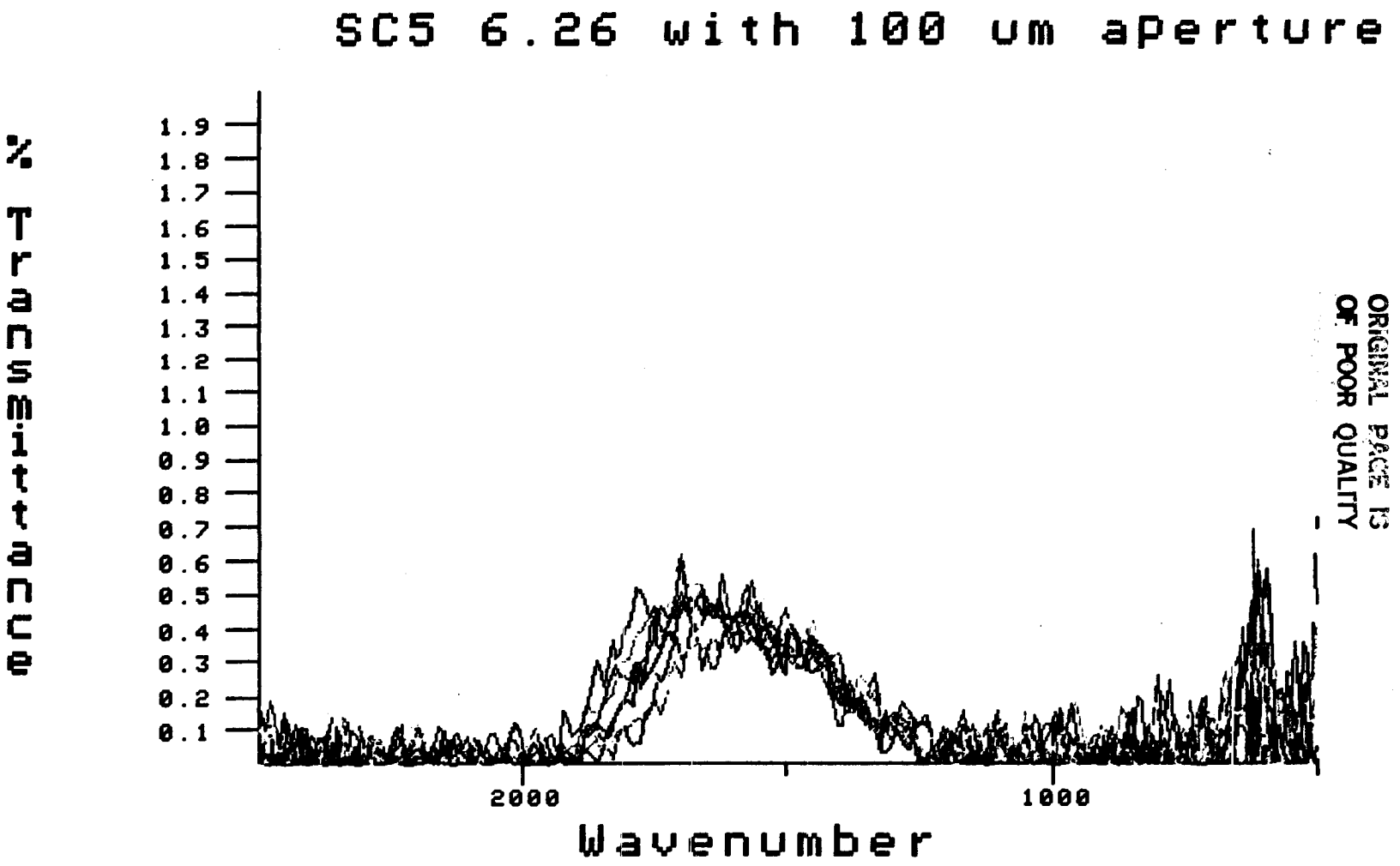

ORIGINAL PAGE IS
OF POOR QUALITY

Figure 12. % Transmittance vs. Wavenumber for the Central Region of Sample SC5-6.26 (as - grown)

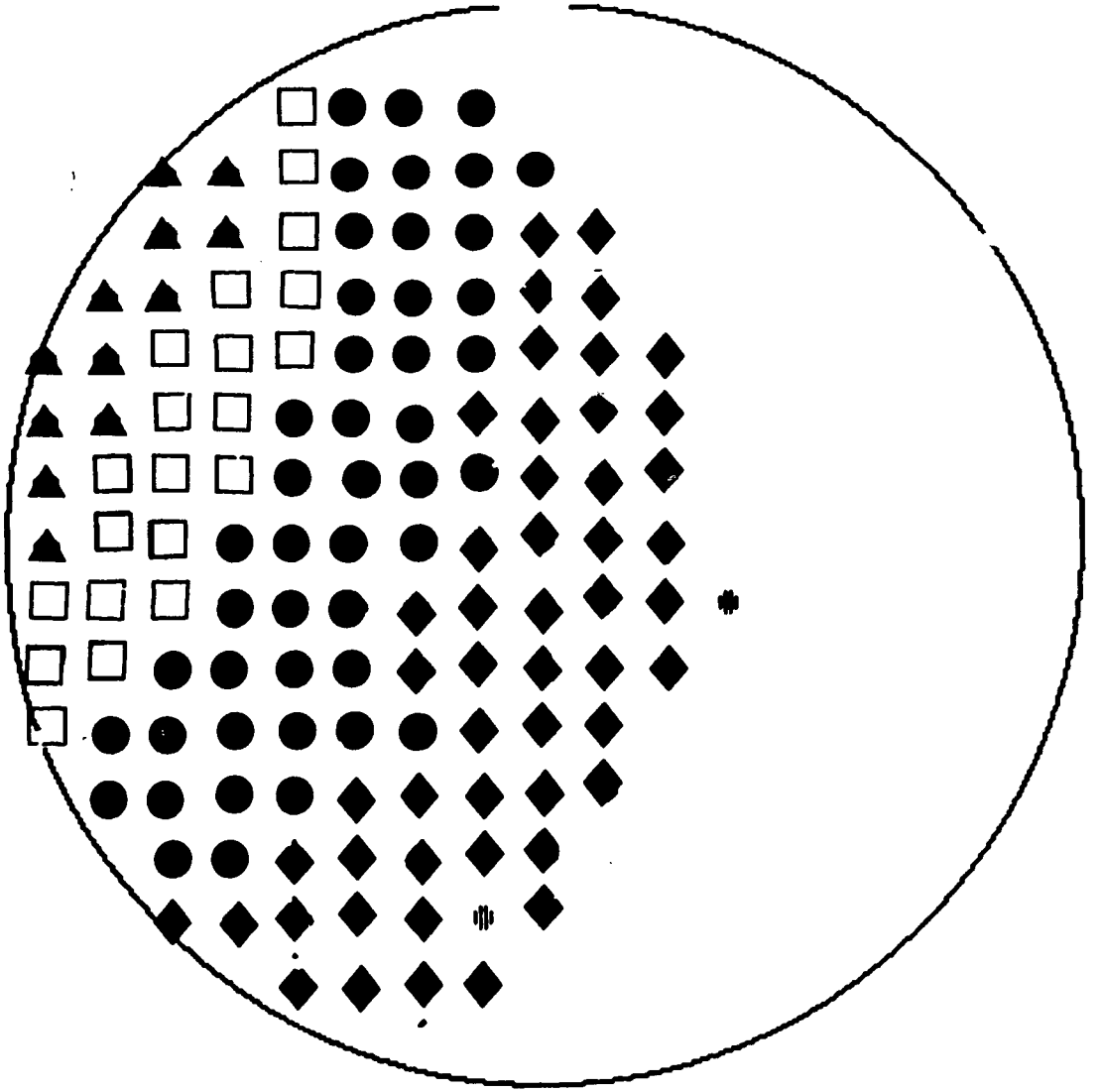

ORIGINAL PAGE IS
OF POOR QUALITY

Figure 13. Wavenumber Contour Map for Sample SC5-6.26

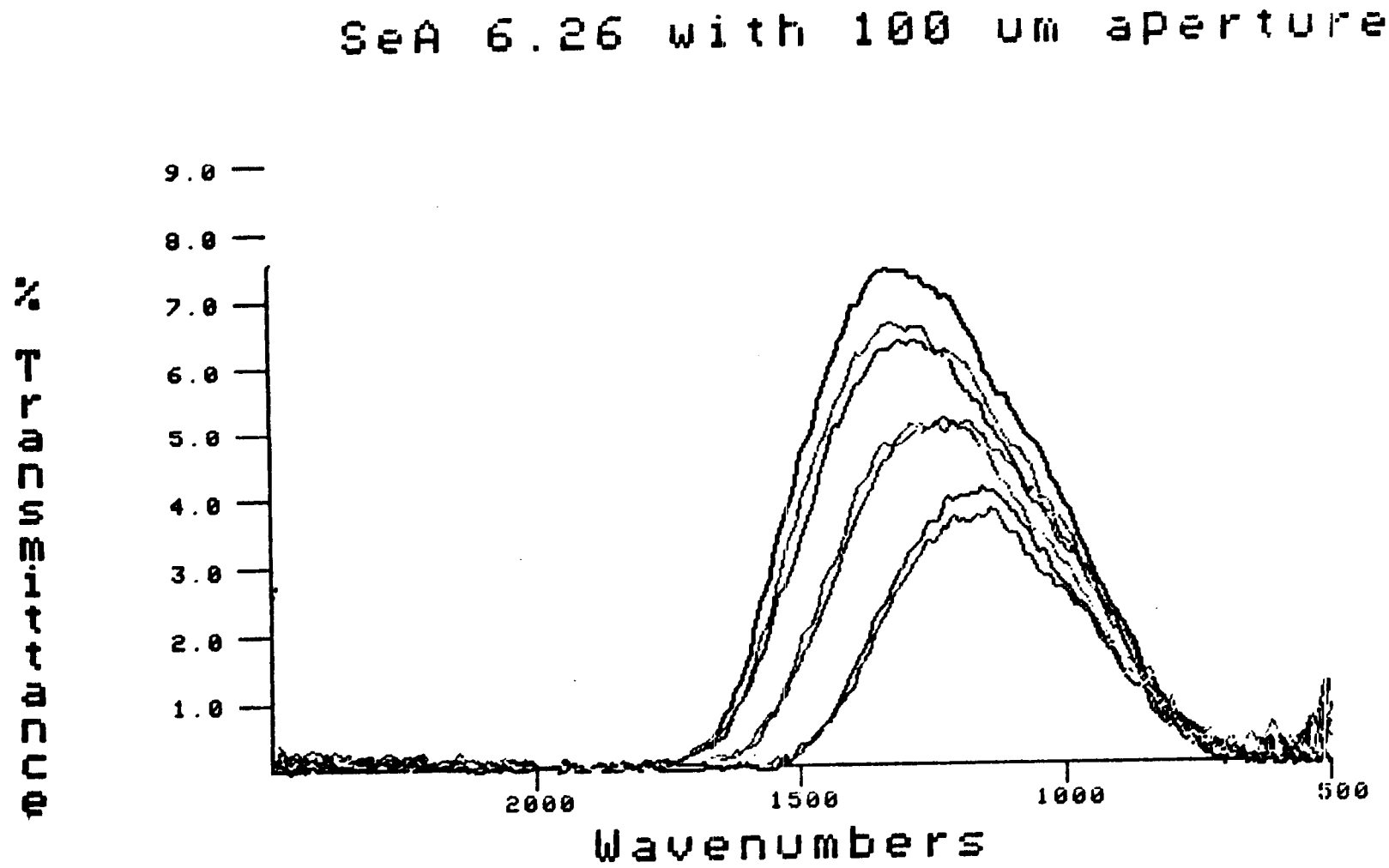

Figure 14. % Transmittance vs. Wavenumber for the Central Region of Sample SC5-6.26 (Annealed 96 hours in Se Vapor)

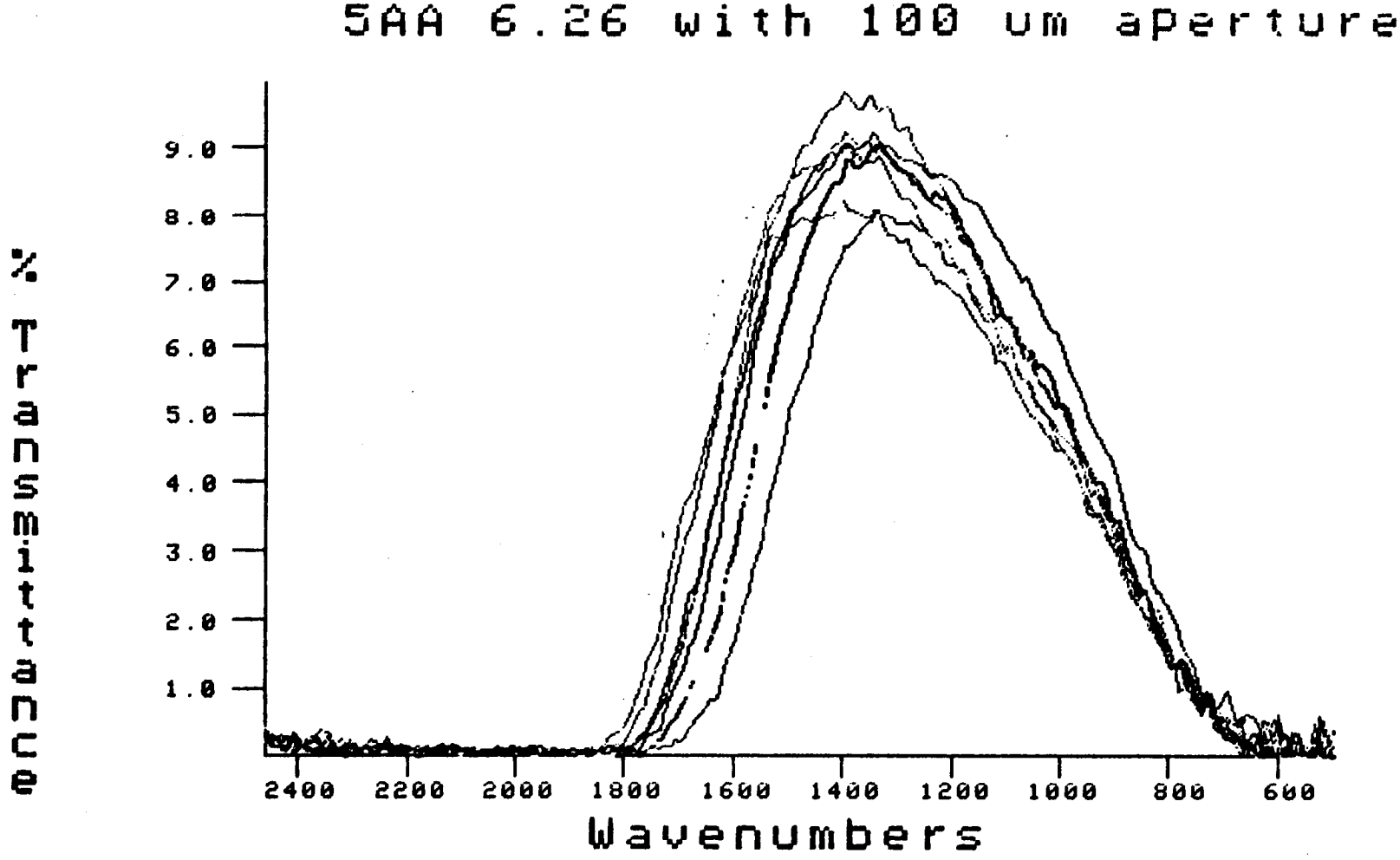

Figure 15. % Transmittance vs. Wavenumber for the Central Region of Sample SC5-6.26 (Annealed $\sim$ 300 hours in Se Vapor)

CONCLUSIONS

As a result of this work, the following conclusions can be made:

1. The effect of growth rate on the axial compositional uniformity appears to be consistent with trends observed in similar II - VI systems. That is, the faster growth rates tend to produce more axially uniform material.

2. Small transients observed in the axial composition profiles indicate that the effective diffusion coefficient may be smaller in this system than in other similar II - VI systems.

3. A slower growth rate was shown to produce a more radially homogeneous material.

4. The carrier concentration in a typical as-grown sample of $Hg_{1-x}Zn_xSe$ is on the order of magnitude of 10^{18} cm^{-3} and appears to be fairly constant as a function of temperature at these high carrier concentrations. The Hall mobility increases as the temperature decreases from 300 to 20K and the resistivity decreases in going from 300 to 20K.

5. Selenium - vapor annealing was effective in reducing the number of native donor defects in $Hg_{1-x}Zn_xSe$ and enhanced the % IR transmission.

6. After annealing in a selenium vapor, the carrier concentration was lower at all temperature compared to the values in the unannealed samples, and was observed to decrease with decreasing temperature. The room temperature mobility remained approximately the same, however the low temperature mobility greatly increased. The low temperature resistivity remained approximately the same with the room temperature resistivity somewhat higher in the annealed samples.

REFERENCES

1. Nelson, D. A., Broerman, J. G., Summers, C. J., and Whitsett, C. R., "Electron Transport in the $Hg_{1-x}Cd_xSe$ Alloy System," Physical Review B, Vol. 18, No. 4, 1658-1672 (1978).

2. Krucheamu, D., "Solid Solutions in Pseudobinary Systems ZnSe-HgSe, ZnTe-HgTe, Revue de Physique, Vol. 8 379-382 (1963).

3. Kot, M. V., and Simashkevich, A. V., "Structure and Electric Properties of the ZnSe-HgSe System," Academy of Sciences Bulletin-Physical Series-USSR, V. 28, 965-968 (1964).

4. Potapov, G. A., Ponomarev, A. I. Gavaleshko, N. P., and Khomyak, V. V., "Shubnikov-de Hass Oscillations in $Zn_xHg_{1-x}Se$".

5. Gavaleshko, N. P., and Khomyak, V. V., "Band Structure and Carrier Scattering Mechanisms in $Zn_xHg_{1-x}Se$," Sov. Phys. Solid State, Vol. 18, No. 10, 1720-1723 (1976).

6. Potapov, G. A., Ponomarev, A. I., Gavaleshko, N. P., and Khomyak, "Galvanomagnetic Effects in $Zn_xHg_{1-x}Se$," Sov. Phys. Semicond. Vol. 13, No. 5, 517-520 (1979).

7. Gavaleshko, N. P. Gorley, P. N., Khomyak, V. V., and Shenderovskii, V. A., "Mechanisms of Current Carrier Scattering in $Zn_xHg_{1-x}Se$," Phys. Stat. Sol. (b) Vol. 98, 463-471 (1980).

8. Gavaleshko, N. P. Khomyak, V. V., Frasunyak, V. M., Parsnchich, L. D., and Parachich, S. Yu., "Energy Band Parameters of $Mg_xHg_{1-x}Te$, $Zn_xHg_{1-x}Se$, and $Cd_xHg_{1-x}Se$ Solid Solutions Determined From the Plasma Reflection Minimum," Sov. Phys. Semiconductors, Vol. 18, No. 9, 967-969 (1984).

9. Leibler, K., Giriat, W., Checinski, K., Wilamowski, Z., and Iwanowski, R., "EPR of Mn^{+2} Ions in Mixed Crystals of $Zn_wHg_{1-w}Se$ and $Zn_mHg_{1-m}Te$," Phys. Stat. Sol. (b), Vol. 55, 447-450 (1973).

10. Lehoczky, S. L., Szofran, F. R., and Martin, B. G., "Advanced Methods for Preparation and Characterization of Infrared Detector Materials," McDonnell Douglas Report MDCQ0717, NASA Contract NAS8-33107 (1980).

11. Lehoczky, S. L., and Szofran, F. R., "Directional Solidification and Characterization of $Hg_{1-x}Cd_xTe$ Alloys," in Materials Processing in the Reduced Gravity Environment of Space, Ed. G. E. Rindone (North - Holland, Amsterdam), 409-420 (1982).

12. Bowman, H. A., Schooner, R. M., and Jones, M. W., J. Res. Natl. Bur. Std., 710, 179 (1967).

13. Van der Pauw, L. J., Philips Res. Rep. Vol. 13, 1 (1958).

Appendix I

Electrical Property Data For SC-5 and SC-6

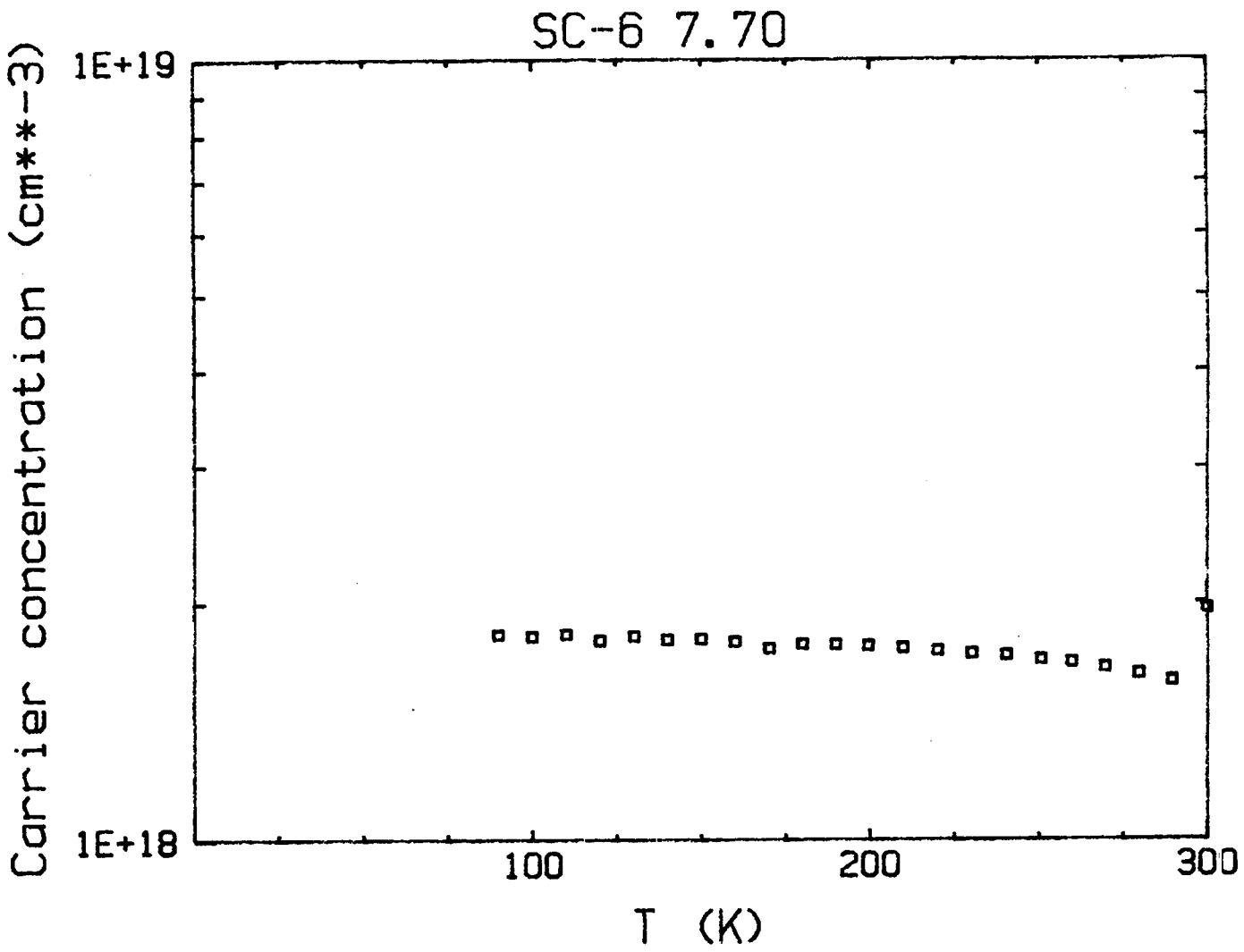

Figure 16. Carrier Concentration as a Function of Temperature for Sample SC6-7.70

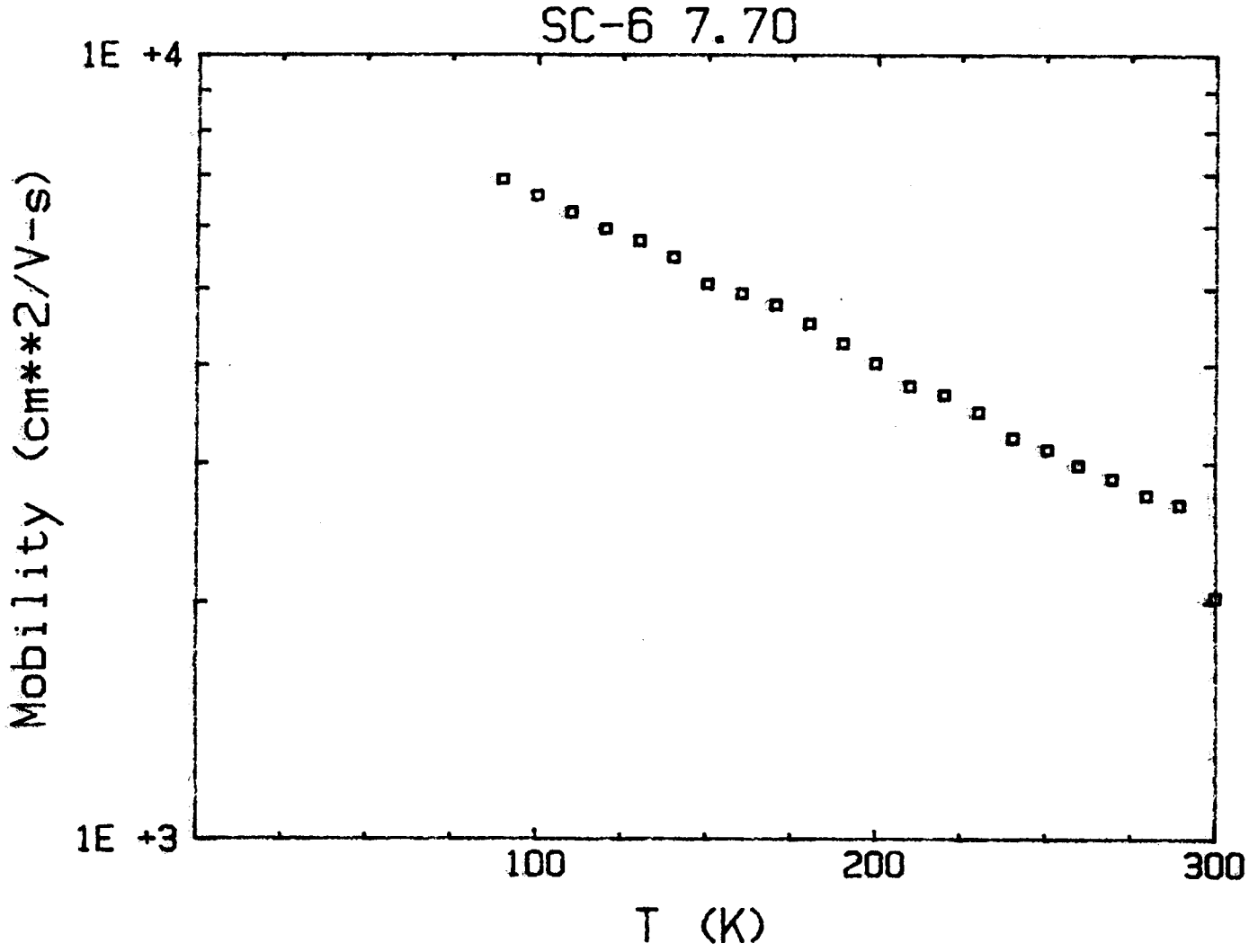

Figure 17. Hall Mobility as a Function of Temperature for Sample SC6-7.70

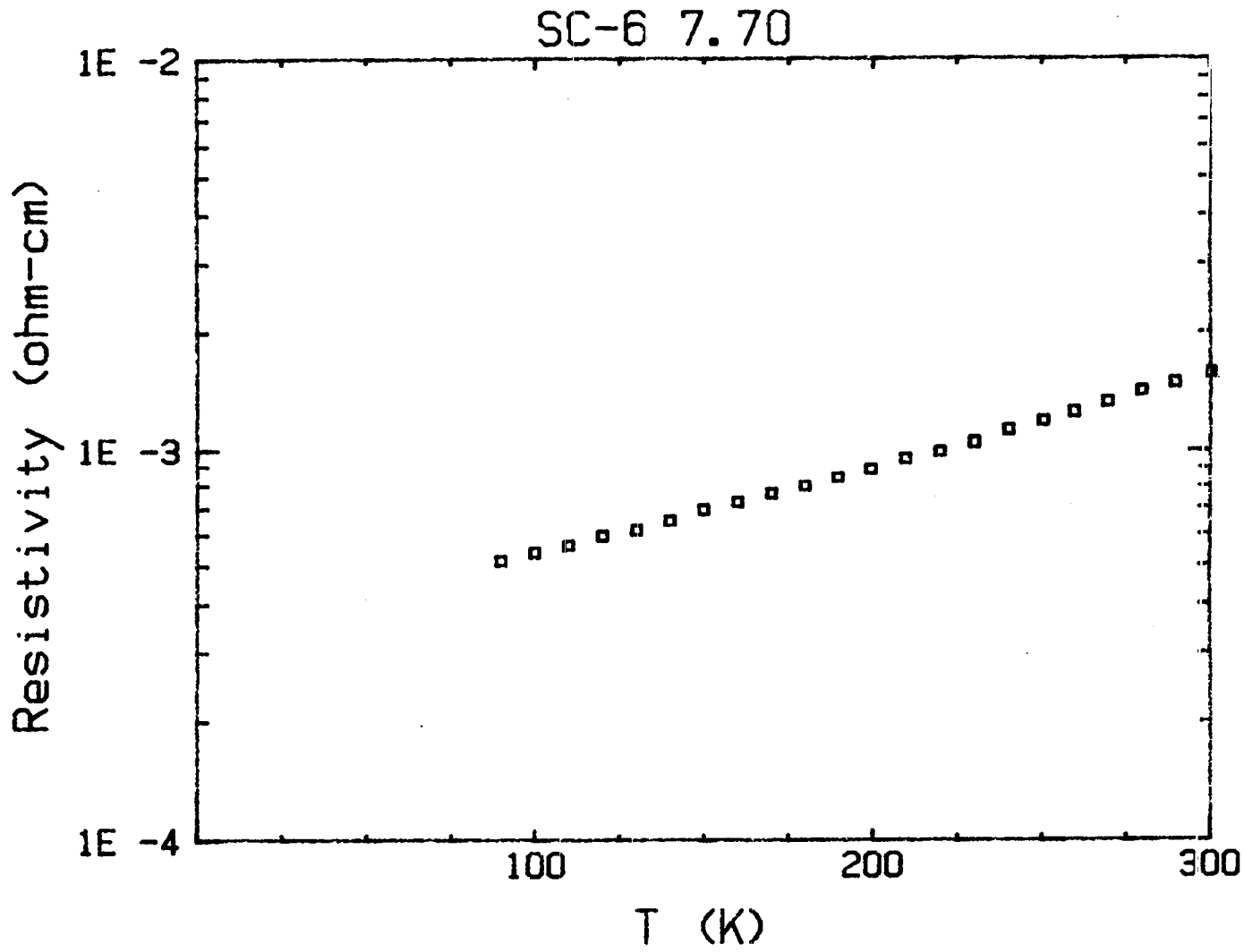

Figure 18. Resistivity as a Function of Temperature for Sample SC6-7.70

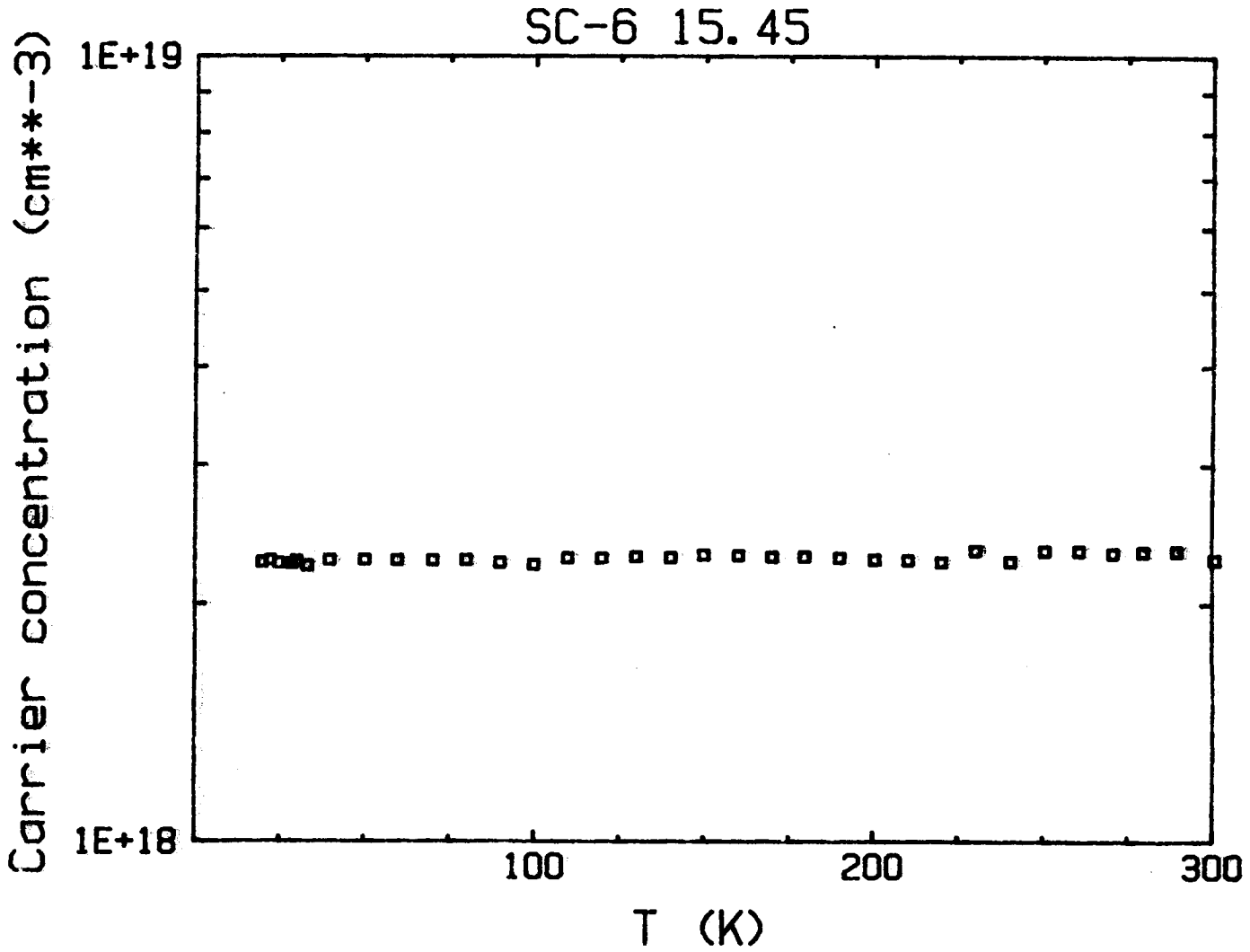

Figure 19. Carrier Concentration as a Function of Temperature for Sample SC6-15.45

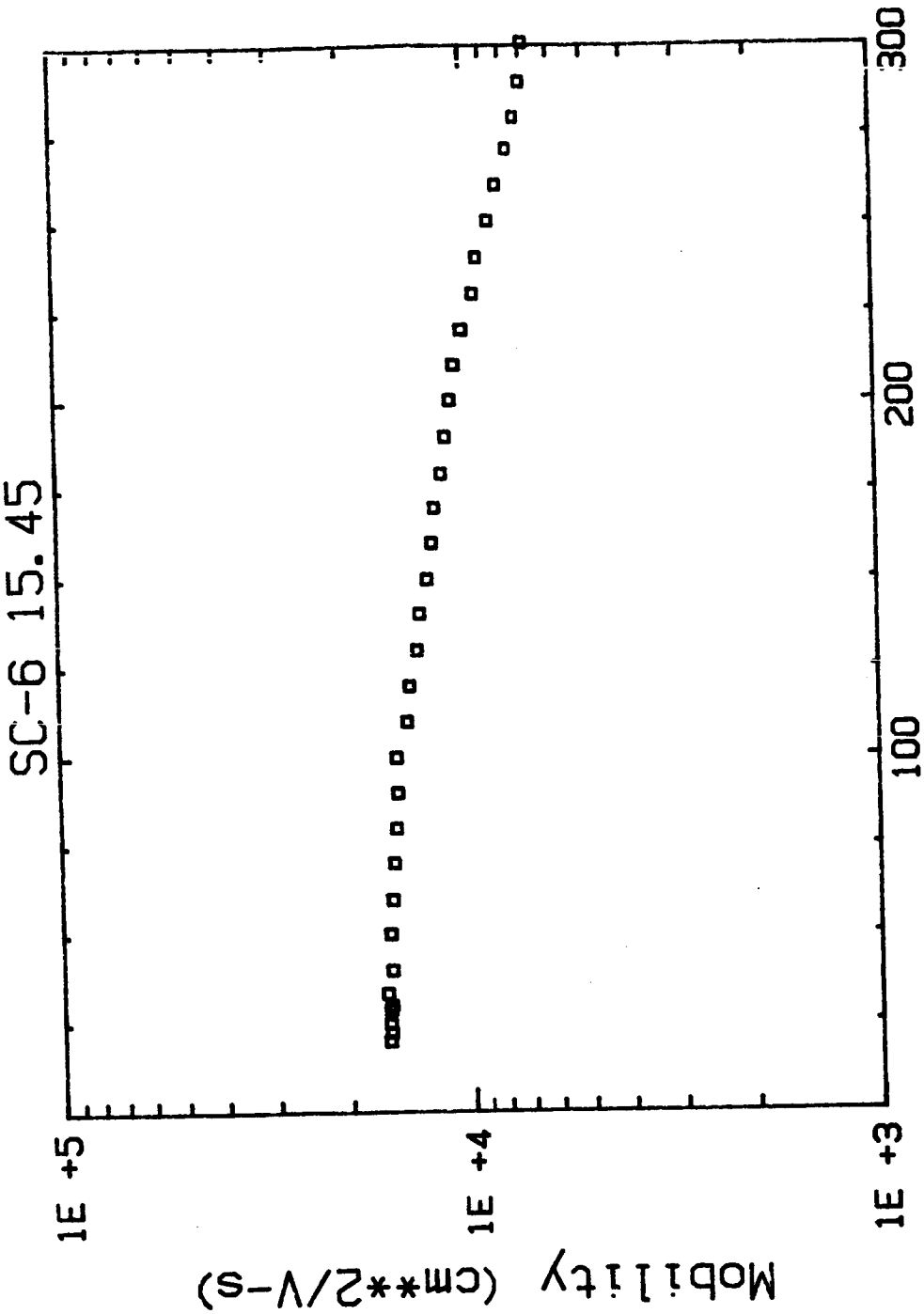

Figure 20. Hall Mobility as a Function of Temperature for Sample SC6-15.45

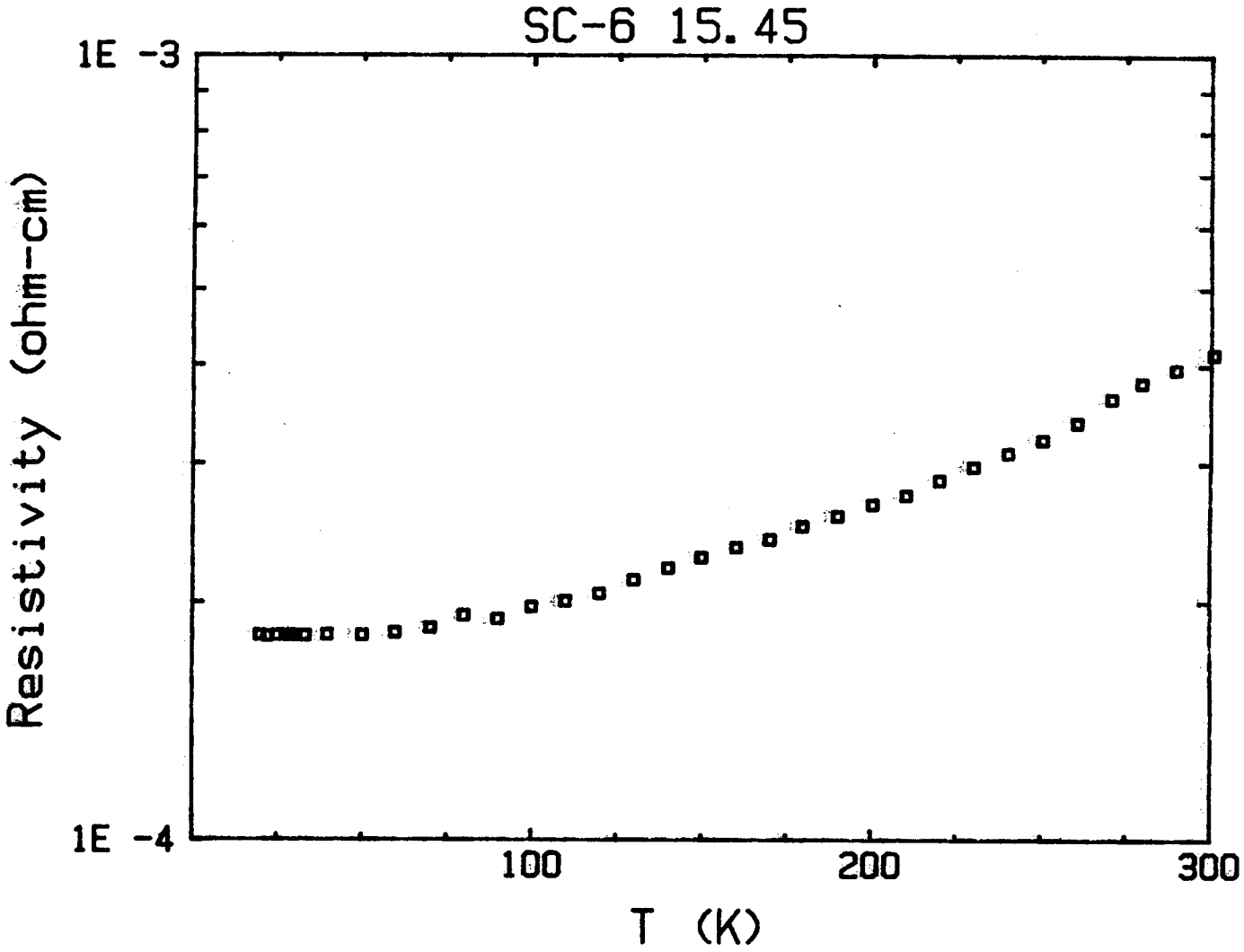

Figure 21, Resistivity as a Function of Temperature for Sample SC6-15.45

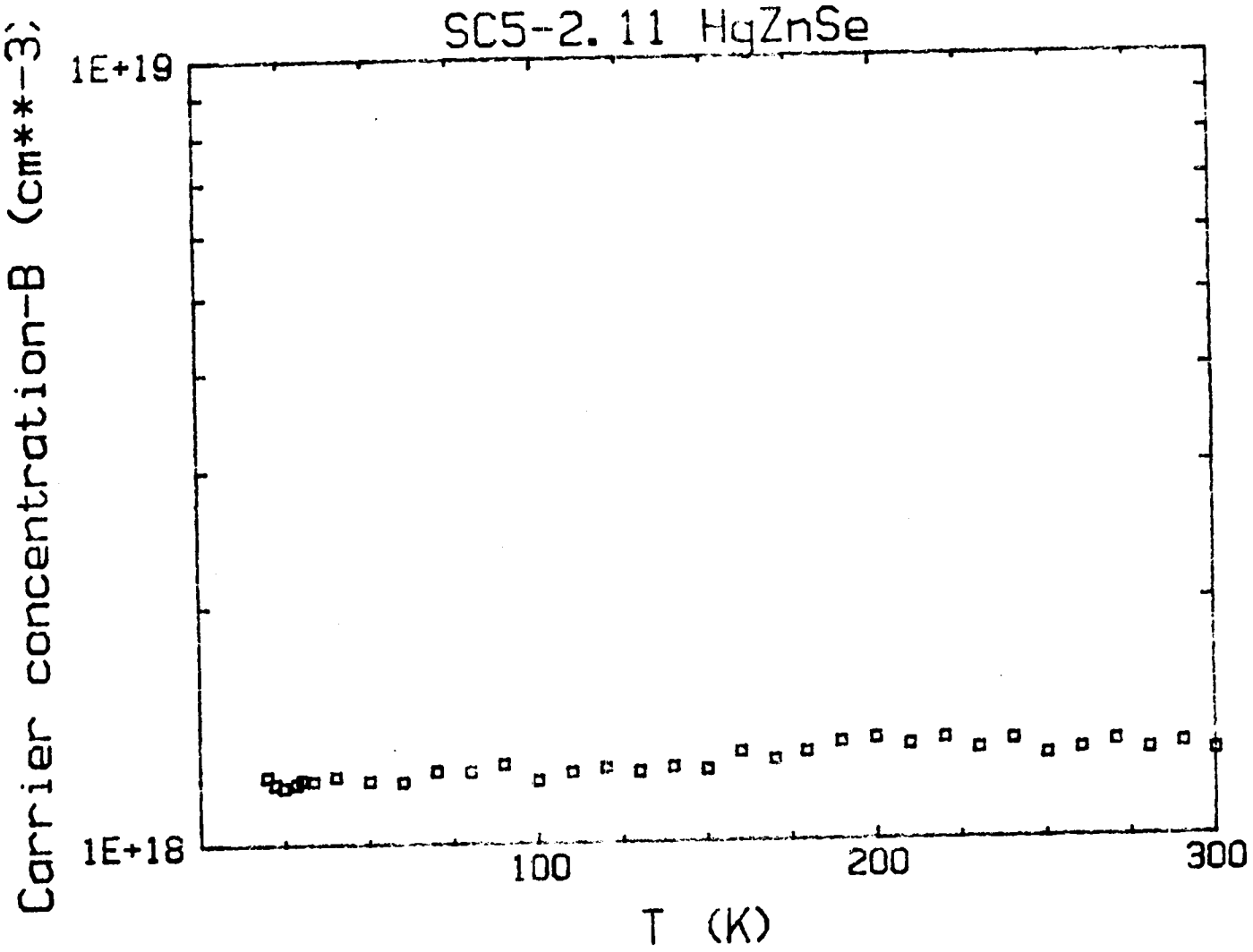

Figure 22. Carrier Concentration as a Function of Temperature for Sample SC5-2.11

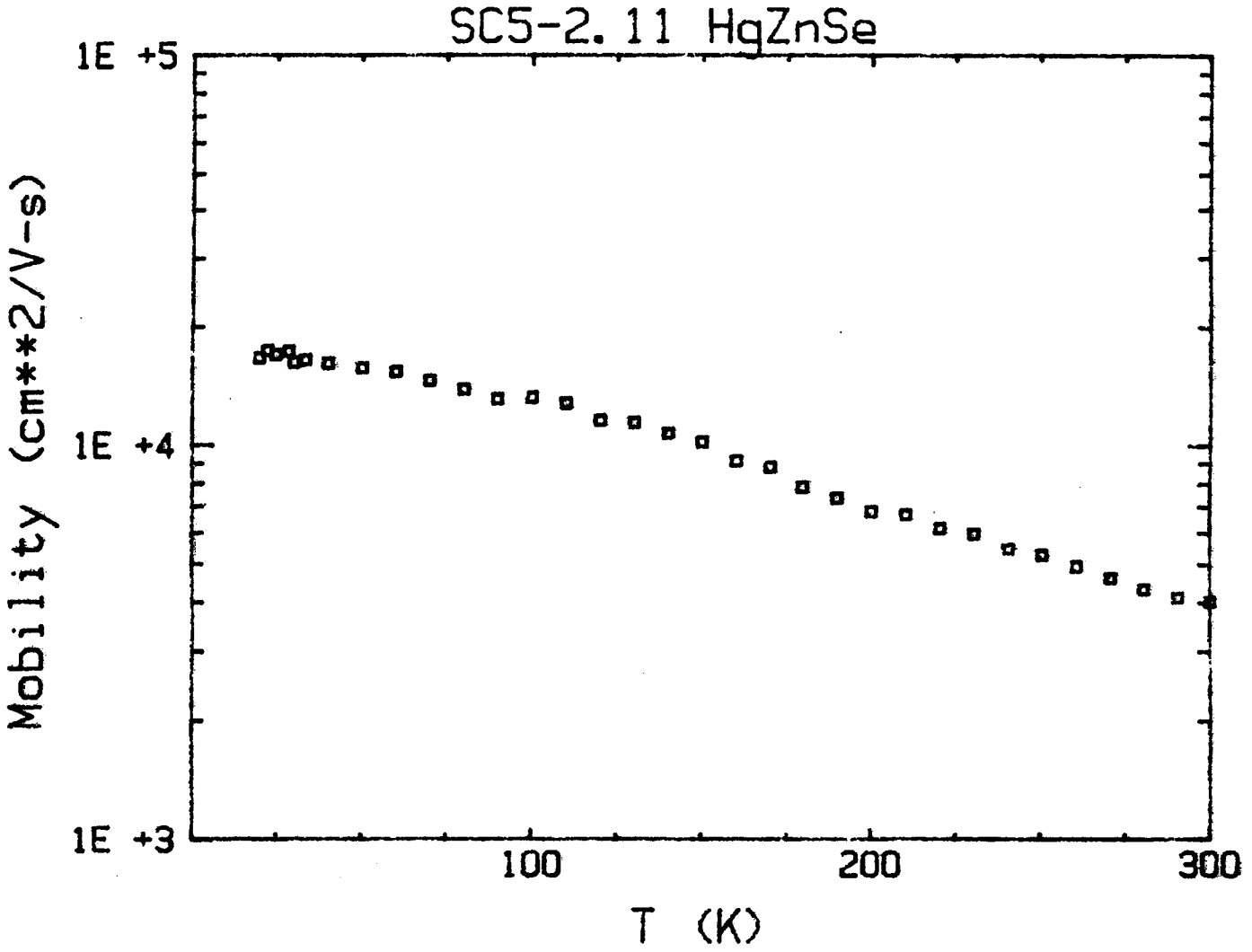

Figure 23. Hall Mobility as a Function of Temperature for Sample SC5-2.11

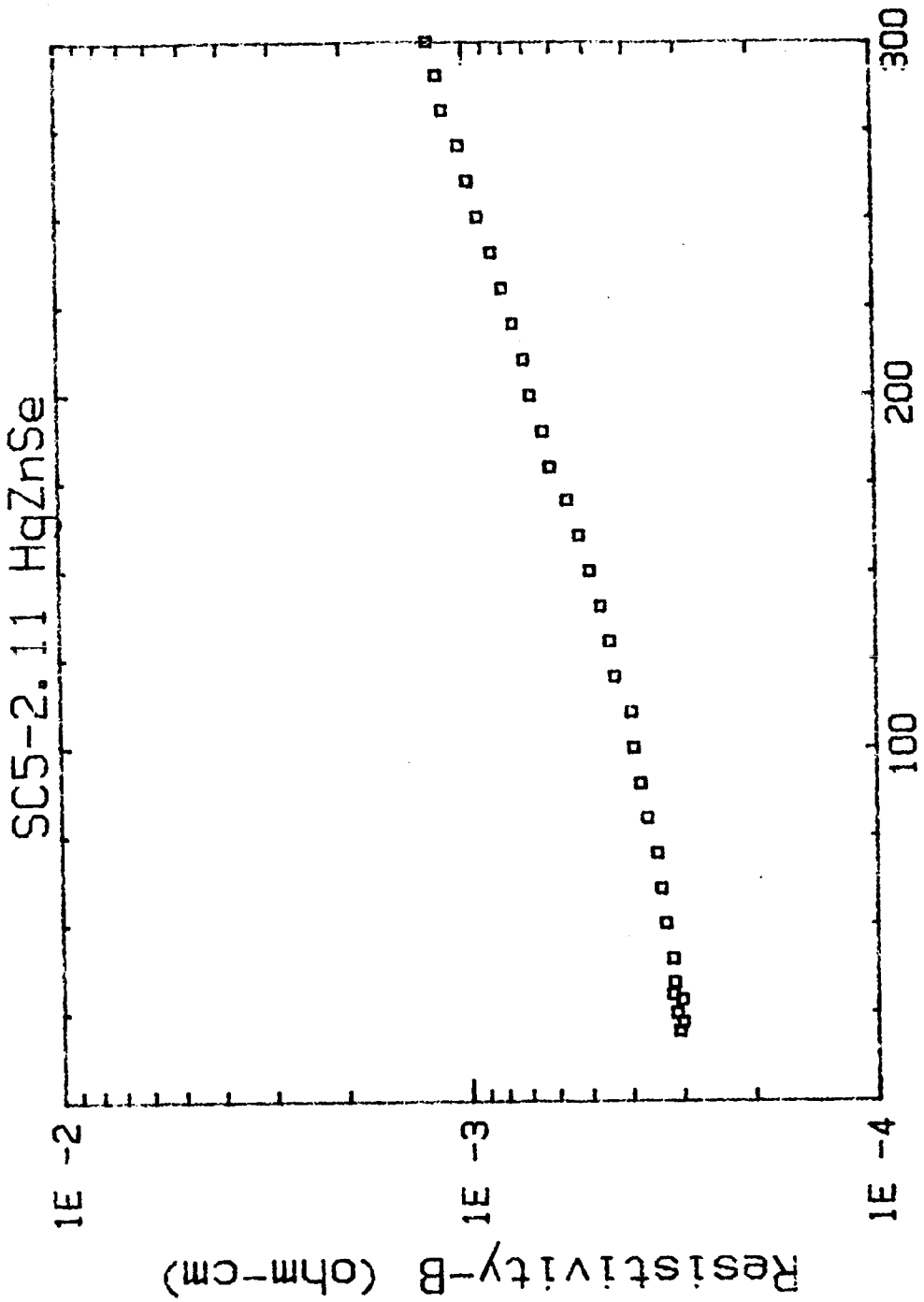

Figure 24. Resistivity as a Function of Temperature for Sample SC5-2.11

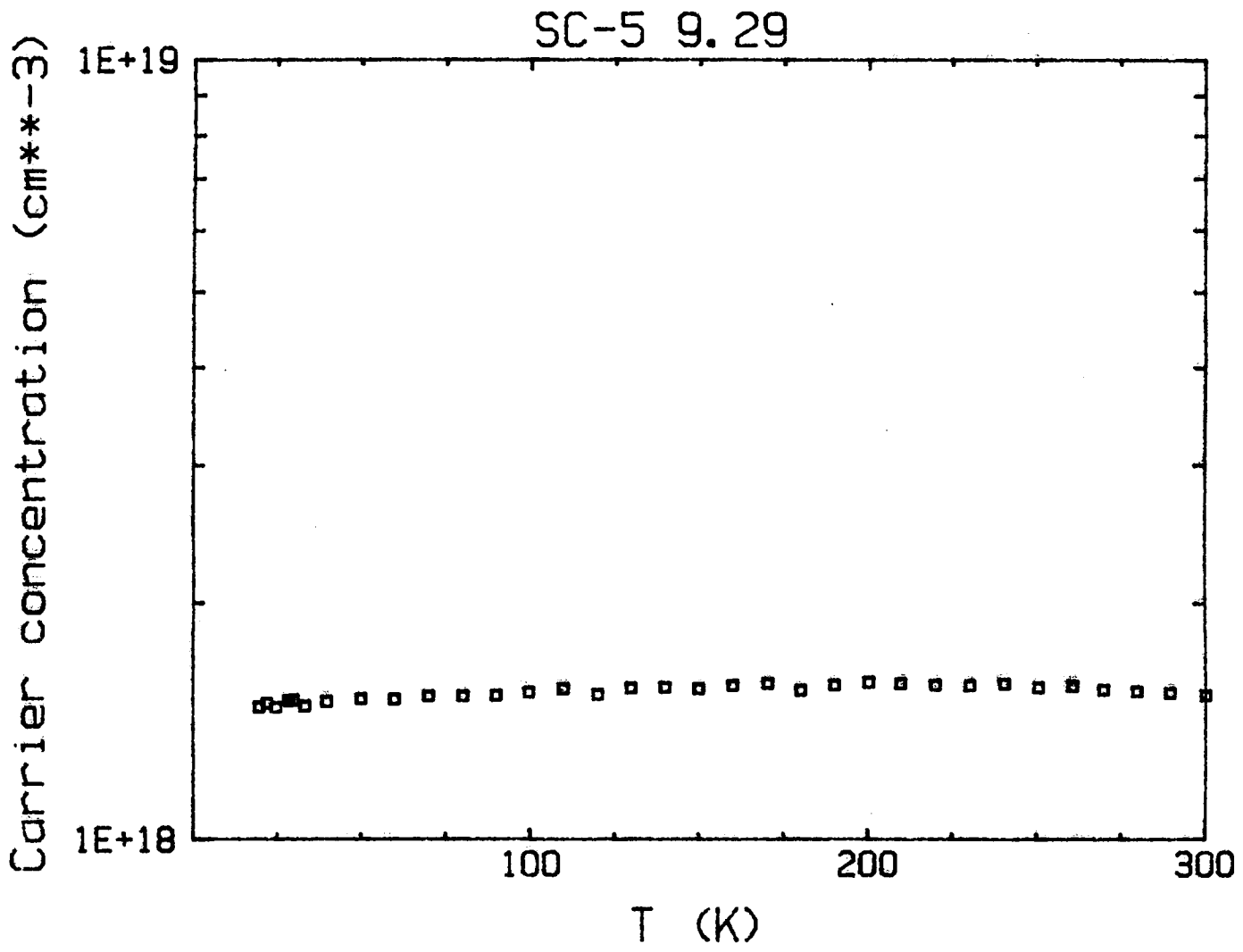

Figure 25. Carrier Concentration as a Function of Temperature for Sample SC5-9.29

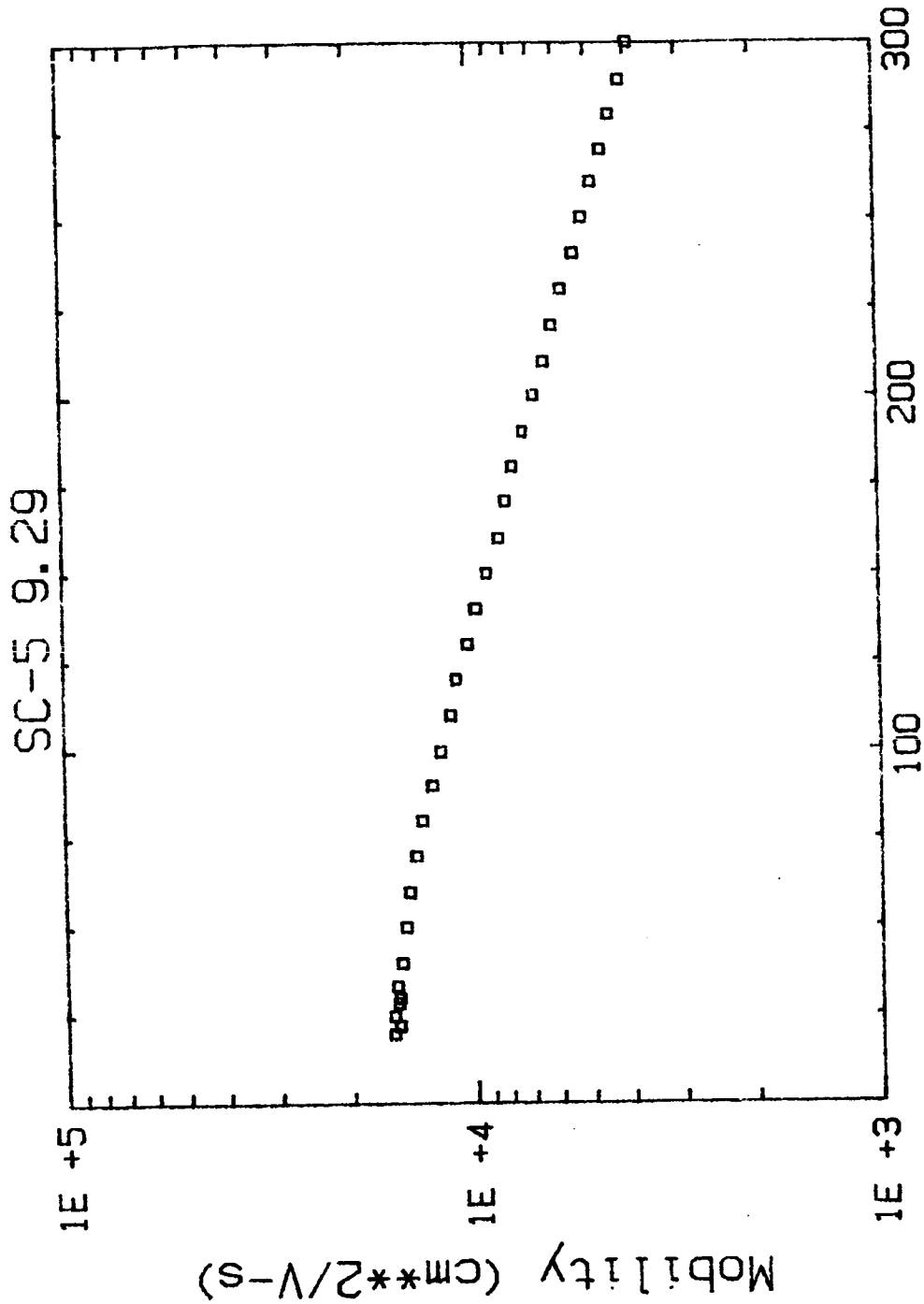

Figure 26. Hall Mobility as a Function of Temperature for Sample SC5-9.29

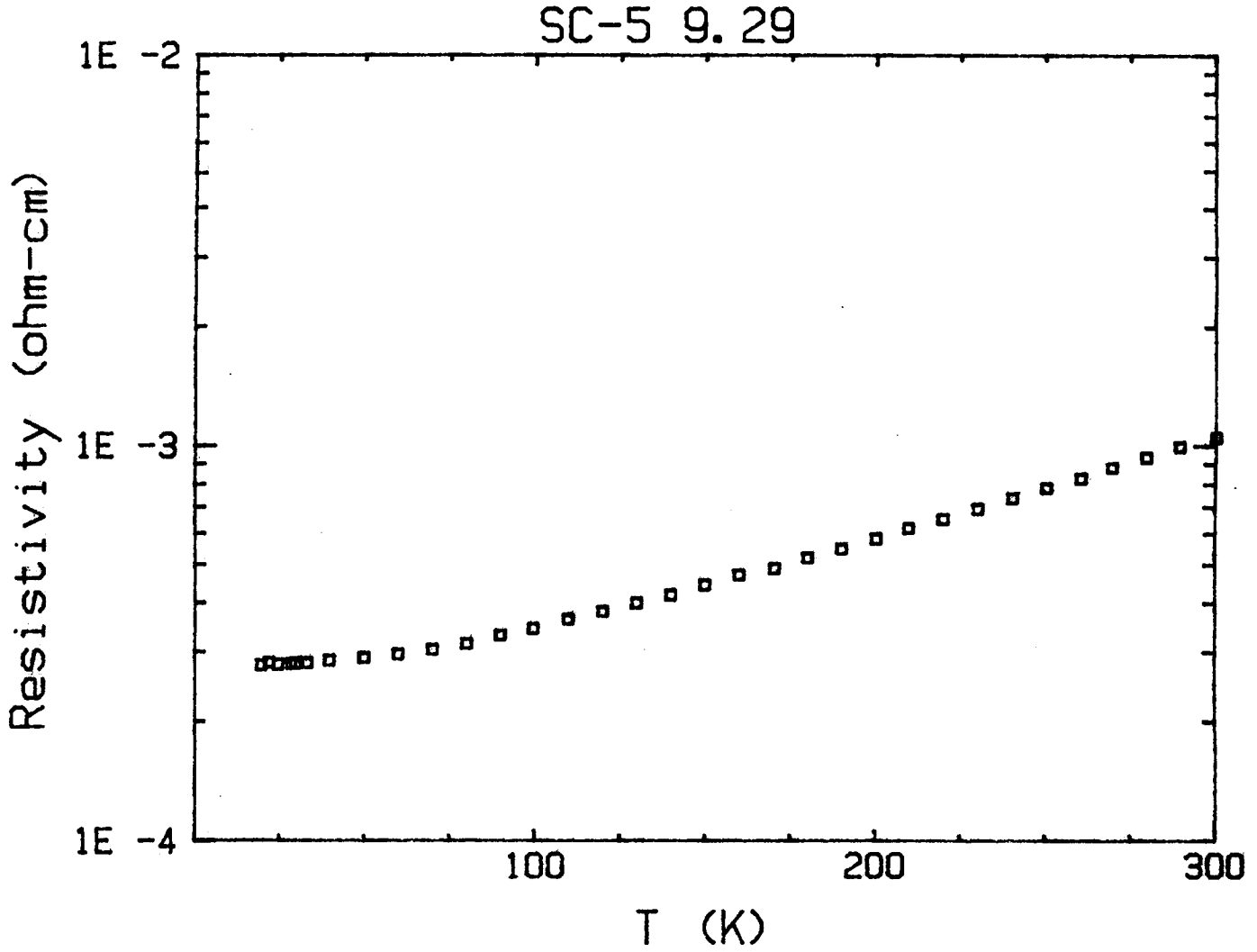

Figure 27. Resistivity as a Function of Temperature for Sample SC5-9.29